RSC Advances

REVIEW

View Article Online
View Journal | View Issue



Cite this: *RSC Adv.*, 2022, **12**, 22722

# Application of nanosonosensitizer materials in cancer sono-dynamic therapy

Chaotao Hu, Biao Hou* and Songlin Xie*

Received 20th June 2022
Accepted 26th July 2022

DOI: 10.1039/d2ra03786f

rsc.li/rsc-advances

Sonodynamic therapy (SDT) is a novel non-invasive treatment for cancer combining low-intensity ultrasound and sonosensitizers. SDT activates sonosensitizers through ultrasound, releasing energy and generating reactive oxygen species to kill tumor cells. Compared with traditional photodynamic therapy (PDT), SDT is a promising anti-cancer therapy with the advantages of better targeting, deeper tissue penetration, and higher focusing ability. With the development and broad application of nanomaterials, novel sonosensitizers with tumor-targeting specificity can deliver to deep tumors and enhance the tumor microenvironment. In this review, we first review the mechanisms of sonodynamic therapy. In addition, we also focus on the current types of sonosensitizers and the latest design strategies of nanomaterials in sonosensitizers. Finally, we summarize the combined strategy of sonodynamic therapy.



## 1. Introduction

Tumors are currently one of the most challenging problems in the medical field.[1] Traditional surgical resection, radiotherapy, and chemotherapy have contraindications, drug resistance, and long-term side effects, seriously affecting patients' quality of life.[2] Some non-invasive treatment modalities, such as photodynamic therapy (PDT) and sonodynamic therapy (SDT), are gradually coming into the limelight. Originally proposed by Japanese scientist Yumita, sonodynamic therapy is a non-invasive tumor treatment technique that originated from photodynamic therapy.[3] Compared with PDT, SDT can penetrate and affect deep tissue lesions. At the same time, ultrasound therapy can precisely target tumor tissues by controlling the frequency, time, and intensity of irradiation to kill cancer cells and minimize damage to surrounding healthy tissues.[4–6]

Current studies have shown that the mechanisms of sonodynamic therapy for tumor treatment are ultrasound cavitation effect, ultrasound thermal effect, oxygen radical theory, apoptosis, autophagy, and the combination of the above mechanisms. Ultrasound activates the sonosensitizer in the cell through the effects of "sonoluminescence" and "acoustic heating," making it in an excited state, and undergoes a series of reactions with surrounding oxygen molecules to produce reactive oxygen species (ROS), mainly singlet oxygen species ($^1O_2$).[7,8] ROS kills tumor cells by inducing apoptosis and synergistically by the physical–mechanical effects of ultrasound.[9,10] SDT can damage the mitochondria of these cells, causing activation of cysteine aspartase, leading to a decrease in mitochondrial membrane potential (MMP) and inducing apoptosis.[11–13] When tumor cells die, they release tumor-associated antigens (TAAs) to induce immunogenic cell death (ICD) to trigger an immune response, enabling SDT to exert subsequent immune anti-tumor responses.[14–17]

Sonosensitizers are an integral part of the SDT process. Sonosensitizers convert acoustic energy into chemical energy through special chemical structures to generate ROS to complete SDT. Therefore, the performance of the sonosensitizer can significantly affect the efficiency of SDT. The ideal sonosensitizer should have good biocompatibility, high bioavailability, and precise tumor targeting.[18–20] Some researchers have designed various nano-drug delivery systems based on proteins, organic polymers, and inorganic materials, combining different nanocarriers and sonosensitizers to improve drug activity and biocompatibility of sonosensitizers.[21] The sonosensitizer is precisely delivered to the tumor site through targeted delivery, thereby improving the intracellular delivery efficiency and acting on the deep site of the tumor, providing a broader application scenario for SDT.[22]

Due to the complex growth mechanism of tumors, it is difficult to achieve the best therapeutic effect with a single treatment method. Combining SDT with other cancer treatments shows excellent potential. For example, SDT combined with photodynamic therapy (PDT), chemotherapy, immunotherapy, and photothermal therapy (PTT) can achieve significant synergistic therapeutic effects.[23–26]

Previous reviews have focused on introducing the mechanism of SDT and a brief review of sonosensitizers, did not focus on the application of SDT in nanomaterials, and failed to summarize the application of SDT in combined tumor therapy. Emerging design strategies for nano-sonosensitizers must also be updated.

*Department of Hand and Foot Microsurgery, The Affiliated Nanhua Hospital, Hengyang Medical College, University of South China, China. E-mail: xiesonglin0929@163.com*

Therefore, in this review, we first review the mechanism of sonodynamic therapy, illustrating the interaction between SDT and ROS. Then, we also discuss the current design, synthesis, characterization, and preliminary biological data of sonosensitizers and the latest design strategies for nano-sonosensitizers to provide references for improving the efficiency of sonodynamic therapy. Finally, we summarize the combination strategies of SDT and other cancer therapies that promise great potential for synergistic anti-cancer treatment.

## 2. The mechanism of SDT

In the past decades, researchers have explored the mechanisms of SDT through many *in vitro* and *in vivo* experiments. The main mechanisms of SDT that have been explored include ultrasound cavitation effect, ROS effect, ultrasound-induced apoptosis, and immune effect. As shown in Fig. 1, it is widely recognized that SDT acts synergistically through multiple mechanisms to cause cell death under ultrasound. However, further studies are still needed to elucidate the exact mechanism of SDT.

### 2.1 Ultrasound cavitation effect theory

The ultrasonic cavitation effect is an important mechanism of SDT.[3,27] The acoustic energy generated by ultrasound causes mechanical pressure changes in the liquid medium, leading to the generation of microbubbles in the tissue fluid, which results in cavitation. In general, ultrasonic cavitation is divided into non-inertial cavitation and inertial cavitation (also known as stable cavitation).[18,28]

Non-inertial cavitation means that when the ultrasound intensity is low, the microbubbles in the liquid do not collapse violently, and their lifespan is relatively long. The microbubbles maintain a stable form in the low-frequency ultrasound field and are forced to oscillate with a small radius, generating radiation and deterrent flows that affect the surrounding cells and biomolecules, increasing cell membrane permeability and making it easier for drugs to enter the cells.[11,27] While inertial cavitation is closely related to ROS generation, inertial cavitation is a relatively strong dynamic process of microbubbles occurring in liquids under high-intensity ultrasound. The microbubbles absorb a large amount of acoustic energy, leading to violent oscillation, expansion, and collapse of the microbubbles. During the collapse, high temperature and pressure are generated, thus releasing a large amount of energy. Therefore, inertial cavitation can induce hydrothermal dissociation and generate hydroxyl radicals. The extreme physical conditions and chemical groups generated by collapse can pose destructive effects on the cytoskeleton, cell membrane structure, and biological enzyme activity and can even kill surrounding cells.[29–32]

In addition, cavitation leads to sonoluminescence (SL) and sonoporation. Through energy transfer, sonoluminescence excites the electron orbitals of the sonosensitizer, and they can produce electron holes ($e^-$–$h^+$), which can pair with the subsequently generated ROS. The generated ROS accumulate in the cytoplasm and organelles, damaging lipids, proteins, and DNA and eventually leading to cell death.[33,34] The sonoporation effect refers to the mechanical effect produced by the oscillation of microbubbles around cells under the action of ultrasound at a specific intensity and frequency. This mechanical oscillation causes the cell membrane to form transient micropores with a 10 minute half-life and a diameter of a few to 150 nanometers. Therefore, the sonoporation effect can increase the permeability of cell membranes and blood vessels and facilitate drug transport.[35,36] Regardless of the type, the final result is conducive to the transport of the drug into the cell, thereby enhancing the therapeutic effect of SDT on tumors.

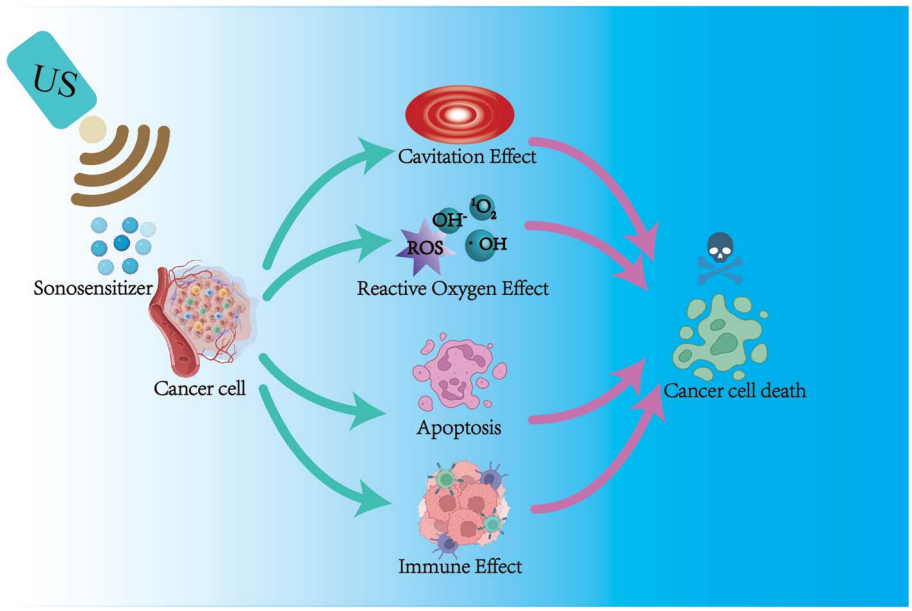


Fig. 1 The schematic diagram of possible mechanisms of SDT.

### 2.2 Reactive oxygen effect

ROS is a class of chemically active oxygen-containing atoms or atomic groups, including singlet oxygen ($^1O_2$), superoxide anion ($^{\bullet}O^{2-}$), hydroxyl radical ($^{\bullet}OH$).[37,38] SDT induces the generation of ROS mainly in two ways. On the one hand, under the cavitation effect, the sonosensitizer is activated from the ground state to the excited state, which can react directly with the surrounding oxygen molecules or other substrate molecules to form oxygen radicals. Subsequently, a large amount of energy is released in the process of returning to the ground state, and the released energy works together with the surrounding oxygen molecules, leading to the production of singlet oxygen. On the other hand, the rupture of microbubbles induced by the cavitation effect can release energy instantaneously, resulting in the cleavage of surrounding water molecules to generate ROS.[39–41]

Singlet oxygen has strong oxidative properties and can reduce the membrane potential of tumor cell mitochondria by capturing electrons, causing damage to the mitochondrial membrane and cytoskeletal atrophy, leading to irreversible destruction of target pathological cells and directly mediating cytotoxicity.[42] Ma *et al.* synthesized three metal 4-methylphenylporphyrin (TTP) complexes (MnTTP, ZnTTP, and TiOTTP) and encapsulated them with human serum albumin (HSA) to form novel nanosensitizers. Under ultrasound, a large amount of singlet oxygen was generated, and the inhibitory effect of singlet oxygen on breast cancer MCF-7 was further confirmed *in vivo* experiments.[43] In addition, oxygen radicals and superoxide anions can also increase the instability of cell membranes through lipid peroxidation chain reactions, disrupt cellular mitochondrial function, and trigger DNA unzipping inducing cellular necrosis or autophagy and ultimately leading to tumor cell death.[44]

Recently, some nanocarriers have been used to enhance the therapeutic efficacy of SDT by improving the sensitivity of sonosensitizers or increasing their accumulation in tumor sites to increase the production of ROS. Yang *et al.* constructed nanosensitizers (collectively termed FA–H@NDs) with perfluoropentane as the core and hematoporphyrin monomethyl ether (HMME) and folate (FA) bound to the surface. When exposed to US irradiation, they can produce excessive ROS, which triggers apoptosis and necrosis of tumor cells/tissues.[45] Therefore, using the ROS therapeutic mechanism of SDT to enhance the efficacy of SDT by increasing the production of ROS is promising cancer therapy.

### 2.3 Ultrasound-induced apoptosis

Apoptosis is a programmed cell death. The most representative regulator, the B-cell lymphoma/leukemia-2 (Bcl-2) gene family and its associated x gene (Bcl-2 associated X, Bax), are the earliest studies related to apoptosis-related genes and also the most critical gene family that regulates apoptosis.[46] SDT can promote apoptosis by regulating the expression levels of the Bcl-2 gene family and its associated x gene (Bcl-2 associated X, Bax), thereby altering the expression levels of downstream Bcl-2 family proteins.[47,48]

Cysteine protease-3 (caspase-3) is an apoptosis-related protease that plays an essential role in cell apoptosis. Jin *et al.* conducted an *in vitro* study on PC-9 cells through a novel porphyrin derivative (BBTPP)-mediated sonodynamic therapy. The results showed that SDT induced ROS production, leading to lipid peroxidation, increasing the expression of apoptosis-related proteins cleaved caspase-9, cleaved caspase-8, Bax, and cleaved caspase-3, as well as inhibiting Bcl-2 expression, and activating extrinsic and intrinsic apoptotic pathways to promote apoptosis in PC-9 cells.[49]

The $Ca^{2+}$ associated apoptotic pathway has also been the focus of research in recent years. SDT can also induce apoptosis in cancer cells by increasing intracellular $Ca^{2+}$ levels, improving mitochondrial membrane permeability, significantly reducing the mitochondrial membrane potential, and merging DNA fragmentation, promoting cytochrome C and the release of apoptotic factors. Multiple factors combine to induce apoptosis in cancer cells.[8,50]

### 2.4 Immune effect

In recent years, researchers have discovered that tumor cells can induce immunogenic cell death (ICD) during SDT and release tumor-associated antigens that trigger an anti-tumor immune response. A series of highly immunostimulatory signals initiate ICD called damage-associated molecular patterns (DAMPs).[51–53]

Cellular immunity is an essential part of anti-tumor immunity, and SDT can better recognize and kill cancer cells by promoting the activator antigen presentation process of T cells.[54] Xie *et al.* designed phase transition nanoparticles (OI_NPs) loaded with perfluoropentane (PFP), indocyanine green (ICG), and oxaliplatin (OXP) to enhance the anti-tumor efficacy and immunological effects of chemotherapy, photodynamic therapy and sonodynamic therapy (PSDT). The results showed that PSDT significantly enhanced the expression of DAMPs, increased T-cell activity, enhanced the immune response of the body, and optimized the anti-tumor therapeutic effect.[55] SDT also promoted the anti-tumor immune effect by upregulating the number of dendritic cells (DCs). Dendritic cells are the most potent specialized antigen-presenting cells (APCs) in the body, which can efficiently take up, process, handle, and sort antigens, present antigenic information to T cells, and initiate antigen-specific T cell responses.[56] Si *et al.* detected ICD markers (ATP, high-mobility group box B1, and calreticulin) and dendritic cell (DC) maturation by flow cytometry. The results showed that nanoparticle-mediated SDT could promote DC maturation by inducing ICD in breast cancer cells to increase the proportion of cytotoxic T cells.[57] Macrophages have a wide range of biological functions and are essential cells involved in innate immunity and adaptive immunity.[58] Ji *et al.* developed mitochondria-targeted and ultrasound-responsive nanoparticles to co-deliver oxygen ($O_2$) and nitric oxide (NO) to enhance SDT and immune responses. SDT was found to promote the maturation of dendritic cells and increase the number of infiltrating immune cells. More importantly, SDT polarized M2 macrophages into M1 phenotype and depleted myeloid-derived suppressor cells to reverse immunosuppression and enhance immune response, thereby improving immune responses to cancer immunotherapy.[59]

The immune response induced by SDT not only promotes the activation and proliferation of the body's immune cells but

also upregulates the expression of cytokines (such as γ-interferon, interleukins, *etc.*), T/B cell costimulatory molecules, and calcium network proteins to enhance the body's anti-tumor immunity. CRT is a highly evolved and conserved intracellular calcium-binding protein. CRT can bind to receptors CD91/LRP1 on the surface of intrinsic immune cells such as macrophages and dendritic cells, and other immune cells to enhance immune responses. The SDT process increases CRT expression on the surface of tumor cells, prompting cytokine release and stimulating the body's specific immune response.[60] The main biological activity of γ-interferon (IFN-γ) is immunomodulatory. In the preparation of tumor vaccines using the immune-activating effect of SDT, Zhang *et al.* found that serum IFN-γ values and IL-2 values were significantly higher, and IL-10 values were significantly lower in mice. This means that SDT can elicit a local immune-inflammatory response in tumors, prompting the conversion of TH2 to TH1 cells. In addition, the infiltration of macrophages in tumor tissues was also significantly increased, with higher expression of CD68 and lower expression of CD163. This indicates that SDT promotes the accumulation of tumor-associated macrophages (TAMs) in tumor lesions and converts TAMs to M1 direction and reduces M2 (with immunosuppressive effect) cells, thereby improving the anti-tumor immune effect.[61] In general, SDT should be considered as a joint action of different mechanisms rather than as a single effect. In the next section, we will list representative examples to discuss the above mechanisms in detail.

# 3. Application of sonosensitizers in SDT

Sonosensitizers are indispensable tools in the SDT process. It converts acoustic energy into chemical energy through a unique chemical structure to generate ROS for SDT. Therefore, the performance of sonosensitizers can significantly affect the efficiency of SDT. Table 1 summarizes the organic small molecule sonosensitizers and their potential sonodynamic mechanisms.

## 3.1 Organic sonosensitizers

**3.1.1 Porphyrins and their derivatives.** Most of the sonosensitizers used in SDT studies are derived from photosensitizers. As the first-generation photosensitizer, porphyrin is widely used in photodynamic therapy, and it is also the first generation sonosensitizer.[62] As shown in Fig. 2, porphyrins include hematoporphyrin (HP), protoporphyrin IX (PpIX), hematoporphyrin monomethyl ether (HMME), and chlorin e6 (Ce6).[63] As early as 1989, Yumita *et al.* treated cell suspensions with hematoporphyrin as a sonosensitizer and then treated sarcoma cells and AH 130 cells with ultrasonic waves at a frequency of 1.92 MHz and different intensities. The results showed that HP combined with ultrasound damaged 99% and 95% of the tumor cells. This pioneered the SDT. The hematoporphyrin used therein became the most classical sonosensitizer.[3] Hematoporphyrin monomethyl ether (HMME) is a second-generation HP-related sensitizer consisting of two monomeric porphyrins. Sun *et al.* investigated the anti-tumor effects of HMME-mediated SDT on endometrial cancer cells. SDT promoted ROS production, induced MMP reduction, and increased intracellular $Ca^{2+}$ concentration. This induced apoptosis in endometrial cancer cells.[64] Protoporphyrin IX (PpIX) is a hematoporphyrin derivative and an essential representative of carboxyl-modified porphyrins. PpIX is converted to the final product heme by chelating with ferrous iron-catalyzed by ferrochelatase. PpIX can also be induced by 5-aminolevulinic acid (ALA). Shono *et al.* enhanced SDT by celecoxib-mediated downregulation of multidrug-resistant protein (MDR1), which elevated cellular PpIX. The presence of PpIX promotes the production of mitochondrial ROS, causing severe damage to tumor cells and selectively destroying glioma stem cells through hydrodynamic shear forces.[65] Phthalocyanines (Pcs) are a group of organic dyes that are electron-rich tetra-pyrrolic macrocycles. The cations on Pcs also help target and deliver sensitizers to negatively charged cancer membranes by opposite charge attraction to enhance efficacy. Nyokong *et al.* prepared cationic morpholine-substituted phthalocyanines conjugated with nitrogen (NGQDs) and nitrogen–sulfur (NSGQDs). The results showed that $^1O_2$ and $^{\cdot}OH$ free radicals were significantly increased after SDT and PSDT treatment, showing the killing effect on breast cancer cells (MCF-7).[66]

**3.1.2 Xanthones.** Xanthones are a family of stains with polycyclic structures, including erythrosine B (EB), rose bengal (RB), eosin, and rhodamine. Erythrosin B is an iodinated derivative of fluorescein with relatively low intrinsic toxicity (Fig. 3A). To investigate whether EB could induce sonodynamic cytotoxicity, Yumita *et al.* found that EB induced by ultrasound

Table 1 Category of sonosensitizer in recent years

| Category | Names | US parameters | Biological model | Ref. |
|---|---|---|---|---|
| Porphyrins and phthalocyanines | HP | 1.92 MHz, 3.18 W $cm^{-2}$, 60 s | Sarcoma 180 cells | 3 |
| | HMME | 1 MHz, 1.0 W $cm^{-2}$, 60 s | Endometrial cancer cell | 64 |
| | PPIX | 1 MHz, 2.0 W $cm^{-2}$, 2 min | Glioma stem cells (GSCs) | 65 |
| | Pcs | 1 MHz, 1.0 W $cm^{-2}$, 10 min | MCF-7 cells | 66 |
| Xanthones | EB | 1.93 MHz, 60 s | Sarcoma 180 cells | 67 |
| | RB | 1 MHz, 2.0 W $cm^{-2}$, 3 min | HepG2 cells | 68 |
| Antineoplastic drugs and NSAIDs | DOX | — | 4T1 cells | 69 |
| | LVFX | 2 MHz, 2.0 W $cm^{-2}$, 30 s | Sarcoma 180 cells | 70 |
| Other sonosensitizers | Curcumin | 3 MHz, 2.0 W $cm^{-2}$, 5 min | HepG2 cells | 71 |
| | HSYA | 1 MHz | Human THP-1 monocytes | 72 |

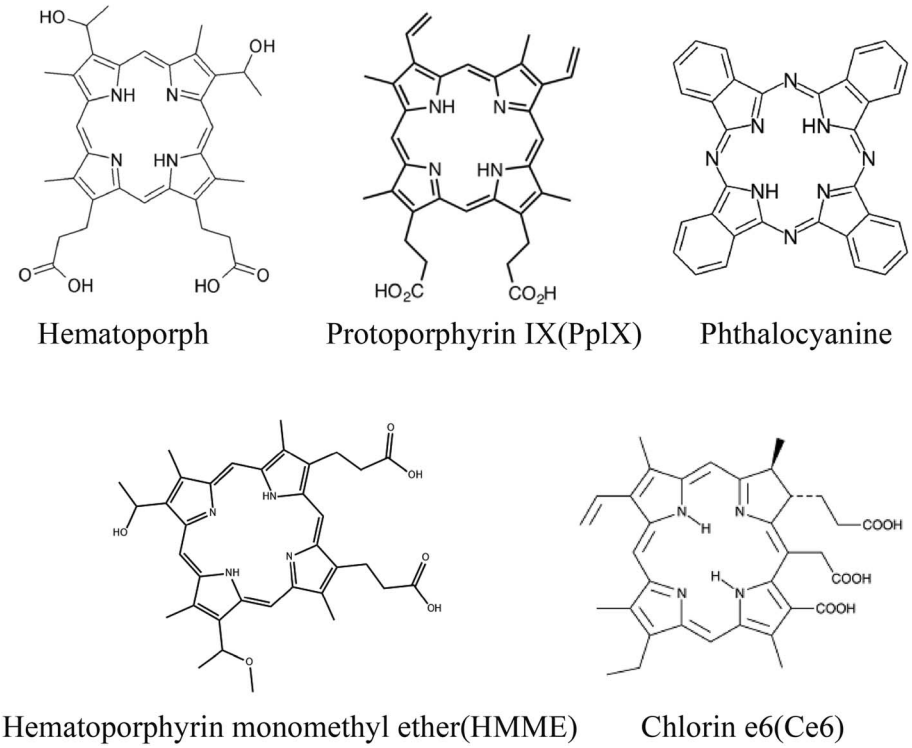


Fig. 2 Chemical structures of porphyrins and their derivatives.

increased the rate of cell damage by 4–5-fold, while no cell damage was observed with EB alone. It was demonstrated that EB enhanced ultrasound-induced tumor cell damage *in vitro* by assessing cellular damage and measuring ESR spectroscopy.[67] RB is a tetrachloro tetraiodide derivative of fluorescein with high singlet oxygen quantum yield under light irradiation (Fig. 3B). This property makes RB an effective photosensitizer capable of inactivating various microorganisms and inducing cancer cell death. Due to RB's high hydrophilicity and poor bioavailability hindering its further development, Chen *et al.* designed and synthesized a series of novel rose bengal derivatives with improved amphiphilicity. The results showed that after the introduction of methoxy polyethylene glycol, RB derivatives showed better tumor cell uptake efficiency than free RB and improved intracellular ROS production for enhanced anti-cancer efficacy.[68]

**3.1.3 Antineoplastic drugs and NSAIDs.** Ultrasound can increase the killing ability of some anti-cancer and chemotherapeutic drugs, such as cisplatin, doxorubicin, *etc.* Doxorubicin is an anthracycline antibiotic commonly used to treat a variety of cancers and can cause DNA damage, apoptosis, production of oxygen radicals and hydroxyl radicals, and enhanced cavitation effect. However, doxorubicin's side effects and systemic toxicity limit the maximum tolerated dose. Nanoparticle-loaded doxorubicin can be used to increase its drug aggregation while reducing toxic off-target effects. An *et al.* prepared a kind of biodegradable hollow polydopamine nanoparticles (P@HP) embedded with platinum nanoparticles (Pt) by co-loading doxorubicin (DOX) and chlorin e6 (Ce6) and modifying with mitochondrial triphenylphosphonium (TPP) (Fig. 3C). Under ultrasound, this nanocomposite material enriches the tumor site by enhancing the permeability and retention effect of solid tumors and then kills tumor cells by inhibiting cellular DNA replication by releasing DOX. Meanwhile, Pt embedded in CDP@HP–T can act as a catalase-like catalyst, triggering the decomposition of endogenous $H_2O_2$ in the tumor, generating $O_2$ *in situ*, alleviating hypoxia at the tumor site, and further improving the effect of SDT. Subsequently, the nanoprobes can carry drugs to target mitochondria through TPP and further improve the anti-tumor therapeutic effect.[69]

Similarly, quinolone NSAIDs and ultrasound also have synergistic anti-cancer effects, including ciprofloxacin (CPFX), gatifloxacin (GFLX), sparfloxacin (SPFX), and levofloxacin (LVFX). The second-generation NSAIDs LVFX showed good anti-cancer activity under US irradiation. Komori *et al.* synthesized LFLX derivatives conjugated with methoxy polyethylene glycol (PEGylated LFLXs) (Fig. 3D). Under ultrasound, the sonodynamic anti-tumor effect of low molecular weight PEGylated LFLXs was superior to that of LFLX, suggesting that PEGylated LFLXs promise anti-tumor compounds as sonosensitizers for SDT.[70]

**3.1.4 Other sonosensitizers.** Due to their unique properties, some natural products can generate sonosensitivity under ultrasound. Curcumin, the main component of turmeric, has anti-tumor effects with low cytotoxicity on normal cells. In addition, curcumin can also act as a sonosensitizer to induce tumor cell apoptosis. To introduce more functions and prepare more efficient sonosensitizers, Zhu *et al.* prepared a curcumin

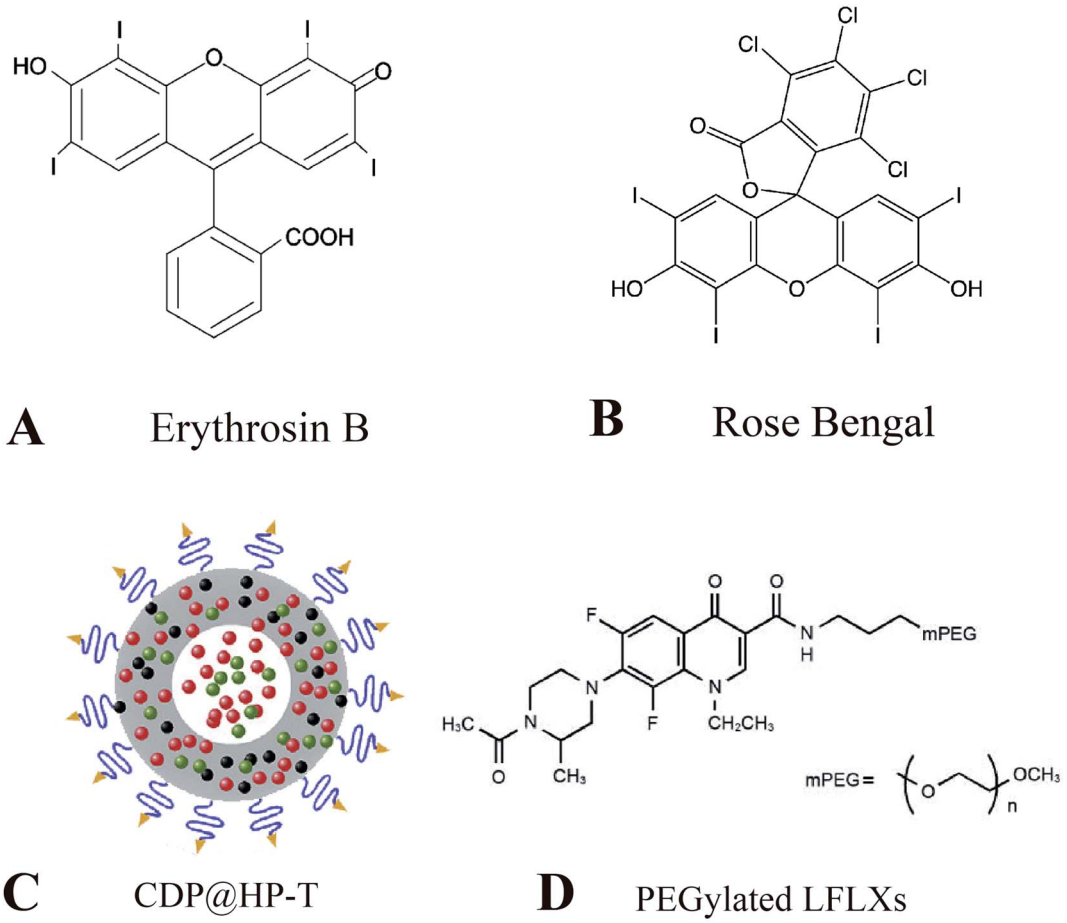


Fig. 3 (A) Chemical structures of erythrosin B; (B) chemical structures of rose bengal; (C) schematic representation of CDP@HP–T; (D) chemical structures of PEGylated LFLXs. (C) Reproduced with permission.[66] Copyright 2020, Elsevier B.V. (D) Reproduced with permission.[67] Copyright 2009, Anticancer Research.

(CUR)-loaded poly(L-lactide-*co*-glycolide) microbubble (CUR–PLGA-MBs). They found that CUR–PLGA-MBs have more pronounced anti-tumor effects in Photodynamic therapy (SPDT) than in sonodynamic therapy (SDT) or photodynamic therapy (PDT) and that CUR–PLGA-MBs is a promising sonic/photosensitizer.[71]

Hydroxy safflower yellow A (HSYA) is the main component of the hydrophilic part of the safflower plant, which has a long history of clinical use in treating cardiovascular disease by intravenous injection. Due to the satisfactory water solubility and high safety profile of HSYA, Jiang *et al.* explored the HSYA-mediated SDT-induced autophagy response *via* the PI3K/AKT/mTOR signaling pathway. ROS generation was significantly increased in the HSYA-SDT group compared to the control group. Furthermore, scavenging of ROS significantly inhibited autophagy, suggesting that HSYA-SDT-induced ROS generation activates autophagy in THP-1 macrophages. These results are consistent with those of other SDT-related studies. Meanwhile, HSYA-SDT-induced autophagy suppressed inflammation through ROS production in THP-1 macrophages.[72]

Although these sonosensitizers all have strong sonodynamic effects, most of the organic sonosensitizers have poor water solubility, unstable properties in the microenvironment, short blood circulation time, and cannot accumulate in large quantities at the tumor site to produce enhanced permeability and retention effect (EPR). The shortcomings limit their further application and development in SDT.[73] Therefore, finding new science and technology to effectively improve the defects of current sonosensitizers and exploring new sonosensitizers is an urgent problem to be solved in the current SDT field.

### 3.2 Nanomaterials loaded with organic sonosensitizers for SDT applications

In recent years, the development of nanotechnology has provided new prospects for the application of traditional sonosensitizers. A series of substances that can be used to prepare nanoparticles have been gradually discovered, such as liposomes, polymers, inorganic materials, and metal materials (Table 2). The application of nanotechnology in SDT mainly has two aspects: on the one hand, physical encapsulation of traditional sonosensitizers in nanocarriers or covalent coupling on nanocarriers can effectively improve the physicochemical properties of traditional sonosensitizers, thereby improving the efficacy of SDT; on the other hand, some inorganic

Table 2 Category of nanosonosensitizer materials in recent years

| Category | Material | Sonosensitizers/drug | Nanoplatform | US parameters | Biological model | Ref. |
|---|---|---|---|---|---|---|
| Polymeric nanomaterials | CS–Ce6–LA NPs | Ce6/docetaxel | CS–Ce6–LA | 1 MHz, 1.0 W $cm^{-2}$ | Melanoma cells | 75 |
| | CS–ADH–Rh–LA NPs | Docetaxel | CS–ADH–Rh–LA | 1.0 W $cm^{-2}$, 3 min | A549 cells | 76 |
| | TCPP–CAT CS/GP | TCPP | CAT–CS/GP | — | CT-26 | 78 |
| | CAT–TCPP/FCS NPs | TCPP | FCS | 3.0 W $cm^{-2}$, 5 min | SV-HUC-1 cells | 79 |
| Liposomal nanomaterials | LEA | Artemether | Liposomes | 1 MHz, 2.0 W $cm^{-2}$, 3 min | HepG2 | 81 |
| | HMME/R837@Lip | HMME/R837 | Liposomes | 1 MHz, 1.5 W $cm^{-2}$, 1 min | 4T1 cells | 25 |
| | ACHL | Ce6, HCQ | Liposomes | 1 MHz, 0.6 W $cm^{-2}$, 60 s | GL261 cells | 47 |
| | FA–MnPs | MnP | Liposomes | 1 MHz, 2.0 W $cm^{-2}$, 3 min | 4T1 cells | 72 |
| Inorganic nanomaterials | HHSN–C/PmAb | Ce6/TPZ | HHSN–C/P-mAb | 1 MHz, 2.0 W $cm^{-2}$ | PC-3 cells | 83 |
| | $GO_x$–$MnO_2$/HMME | HMME | $GO_x$–$MnO_2$ | 1.0 W $cm^{-2}$, 1 min | MCF-7 cells | 84 |
| | Pt–CuS–TAPP Janus | TAPP | Pt–CuS Janus | 1 MHz, 1.0 W $cm^{-2}$ | CT-26 | 85 |
| | HP–HIONs@PDA–PEG | HP | HIONs@PDA–PEG | 1 MHz, 1.5 W $cm^{-2}$, 10 min | PC-3 cells | 86 |
| | BSO–TCPP–Fe@$CaCO_3$ | TCPP | BSO–Fe@$CaCO_3$ | — | 4T1 cells | 87 |
| Titanium dioxide nanomaterials | $TiO_2$ | $TiO_2$ | $TiO_2$ | 39 kHz, 200 W, 60 min | — | 89 |
| | $TiO_2$ | $TiO_2$ | $TiO_2$ | 1 MHz, 0.5 W $cm^{-2}$, 10 s | C32 | 90 |
| | Au NPL@$TiO_2$ | Au NPLs | $TiO_2$ | 3 MHz, 0.5 W $cm^{-2}$, 4 min | HeLa cells | 91 |
| | CCM-HMTNPs/HCQ | HCQ | HMTNPs | 1 MHz, 30 s | MCF-7 cells | 92 |
| | PEG–$TiO_{1+x}$ NRs | $TiO_{1+x}$ NRs | $TiO_{1+x}$ NRs | 40 kHz, 5 min | 4T1 cells | 93 |
| | $TiO_2$/C | $TiO_2$/C | $TiO_2$/C | 1 MHz, 0.5 W $cm^{-2}$, 1 min | Panc02 cells | 94 |
| | COF-$TiO_2$ NPs | COF-$TiO_2$ NPs | COF-$TiO_2$ NPs | 1 MHz, 1.5 W $cm^{-2}$, 4 min | 4T1 cells | 95 |
| Transition metal oxide nanomaterials | $MnWO_x$–PEG | $MnWO_x$–PEG | $MnWO_x$–PEG | 40 kHz, 3 W $cm^{-2}$, 2 min | 4T1 cells | 96 |
| | Janus Au–MnO | Janus Au–MnO | Janus Au–MnO | 1 MHz, 2.0 W $cm^{-2}$, 10 min | MCF-7 cells | 97 |
| | MOF-DHMS | DHMS | DHMS | 1 MHz, 0.6 W $cm^{-2}$, 60 s | — | 98 |
| Noble metal nanomaterials | Cu–Cy | Cu–Cy | Cu–Cy | 1 MHz, 2.0 W $cm^{-2}$, 3 min | MCF-7 cells | 99 |
| | Au@BP NPs | Au NPs | Au@BP NPs | — | 4T1 cells | 100 |
| | $PtCu_3$ nanocages | $PtCu_3$ nanocages | $PtCu_3$ nanocages | 35 kHz, 3.0 W $cm^{-2}$, 1 min | 4T1 cells | 102 |
| | Fe–$VS_2$PEG NSs | Fe–$VS_2$ NSs | Fe–$VS_2$PEG NSs | 40 kHz, 4.5 W $cm^{-2}$, 5 min | 4T1 cells | 103 |
| Carbon-based nanomaterials | $MnO_x$/$TiO_2$–GR | GR, $TiO_2$ | $MnO_x$/$TiO_2$–GR | 1.0 MHz, 1.0 W $cm^{-2}$, 5 min | 4T1 cells | 105 |
| | PPy@MWCNTs | PPy@MWCNTs | PPy@MWCNTs | 1.0 MHz, 1.0 W $cm^{-2}$, 1 min | C540 cells | 106 |
| | FA–N-GQD | N-GQD | FA–N-GQD | 1.0 MHz, 2.5 W $cm^{-2}$, 1 min | MDA-MB-231 | 107 |

nanomaterials have good sonosensitivity properties and can be directly used as sonosensitizers in the research of SDT.[10]

**3.2.1 Polymeric nanomaterials loaded with organic small molecule sonosensitizers.** Polymer nanoparticles have great potential in the targeted delivery of drugs and imaging contrast agents and have been widely used in the biomedical field. Combining traditional organic sonosensitizers and polymers to form composite nanoparticles through self-assembly is an effective way to improve the bioavailability and targeting of these small organic molecules.[74]

To increase cellular uptake of drugs and improve the stability and monodisperse form of nanoparticles, Liu *et al.* designed a novel redox/enzyme/ultrasound responsive chondroitin sulfate–chlorin e6–lipoic acid nanoplatform loaded with doxorubicin. Chlorin e6 (Ce6) was used as a sonosensitizer, grafted onto the chondroitin sulfate (CS) backbone, and then modified with LA to synthesize ultrasound-responsive conjugates (Fig. 4A). When delivered to the intracellular compartment, the disulfide bonds are rapidly dissociated by GSH, resulting in decrosslinking and drug release of the nanoparticles. They

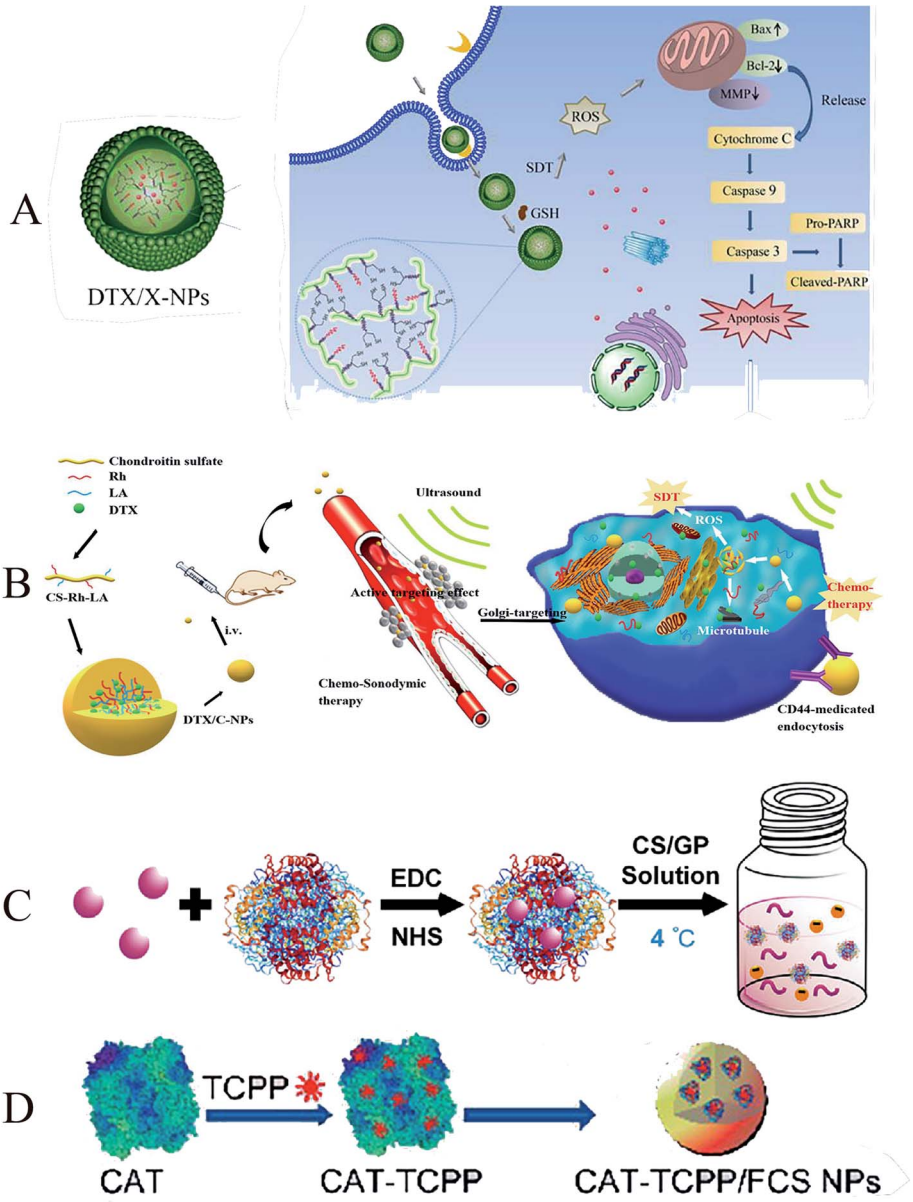


Fig. 4 (A) Illustration of the formation, tumor cellular accumulation and rapid dissociation, cell apoptosis mechanism; (B) synthesis and self-assembly of DTX/C-NPs and illustration of the combined chemo-SDT therapy of the redox/ultrasound-responsive nanoparticles; (C) the scheme demonstrating the thermotriggered gelation process of TCPP–CAT CS/GP hydrogel in tumors of mice; (D) schematic illustration of CAT–TCPP/FCS NPs. (A) Reproduced with permission.[72] Copyright 2018, Elsevier B.V. (B) Reproduced with permission.[73] Copyright 2021, BioMed Central Ltd. (C) Reproduced with permission.[75] Copyright 2020, WILEY-VCH. (D) Reproduced with permission.[76] Copyright 2020, American Chemical Society.

focused on the anti-tumor and proapoptotic mechanisms of Ce6-mediated SDT on melanoma cells. They found that reversibly cross-linked nanoparticles (X-NPs) could generate ROS, reverse mitochondrial membrane potentials (MMPs), and mediate apoptosis through the mitochondria-caspase pathway. Reversibly cross-linked nanoparticles enhance anti-tumor efficiency through chemo-sonodynamic induced apoptosis and death combined with immune activation.[75] Similarly, Zhang *et al.* formed an amphiphilic self-assembled nanoplatform by grafting Rhine (Rh) onto the chondroitin sulfate backbone and using lipoic acid (LA) as a cross-linking agent (Fig. 4B). It can rapidly release encapsulated drugs in the highly reducing environment of the cytoplasm. The nanoparticles successfully enhanced ROS production in a time- and concentration-dependent manner after entering A549 cells, which could effectively inhibit the invasion and migration of cancer cells. The release of DTX may play an important role in SDT by inducing G2/M phase arrest in mitotic cell division and disrupting the microtubule structure of tumor cells. The presence of Rhine can induce apoptosis, change mitochondrial membrane potential, enhance the expression of apoptosis-related proteins, and enhance the anti-tumor effect of SDT.[76]

The hypoxic microenvironment of solid tumors can severely limit the therapeutic efficacy of SDT. Some researchers have developed a new nano-drug delivery platform by self-assembling sonosensitizers and polymers. It can promote the production of $O_2$ from endogenous $H_2O_2$ at the tumor site, thereby alleviating the hypoxic state of the tumor site, promoting the production of ROS, and improving the effectiveness of SDT.[77] To overcome this deficiency, She *et al.* developed a thermally-triggered *in situ* hydrogel system in which catalase (CAT) conjugated with sonosensitizer *meso*-tetra(4-carboxyphenyl)porphine (TCPP) is mixed into chitosan (CS) and beta-glycerol phosphate disodium (GP) to form the precursor solution (Fig. 4C). After the precursor solution was injected into the tumor, the increase in temperature could turn the sol into a gel. Under ultrasound, local TCPP–CAT generates ROS and promotes the efficacy of SDT in tumor killing by triggering the decomposition of endogenous $H_2O_2$ to produce $O_2$, which in turn continuously improves the hypoxic tumor microenvironment.[78] In a later study, a similar novel polymeric nano-drug delivery material was designed by Li *et al.*, who developed a transmucosal oxygen self-producing SDT nanoplatform to achieve high-efficiency SDT targeting BCa (Fig. 4D). In this system, fluorinated chitosan (FCS) is synthesized as a highly effective nontoxic transmucosal delivery carrier to assemble with *meso*-tetra(4-carboxyphenyl)porphin conjugated catalase (CAT–TCPP). CAT–TCPP/FCS nanoparticles exhibited significantly improved transmucosal and intratumoral penetration capacities in the bladder, where catalase catalyzes the production of oxygen from tumor endogenous $H_2O_2$, enhancing the therapeutic efficacy of tumors.[79]

In conclusion, the utilization and targeting of a single organic small molecule sonosensitizer are limited, and the use of polymer nanomaterials as carriers of traditional sonosensitizers has promising applications in the field of SDT.

**3.2.2 Liposomal nanomaterials loaded with organic small molecule sonosensitizers.** Researchers developed nanoliposomes as carriers to improve the biostability and target site accumulation of sonosensitizers. Liposomal nano-drug carriers are widely used in SDT because of their excellent biocompatibility, degradability, and stability. Nanoliposomes are usually composed of phospholipids with a bilayer structure and are effective drug carriers.[80]

Chen *et al.* prepared a nanosensitizer with artemether encapsulated in liposomes (LEA). The results showed that LEA-mediated SDT induced a $70.0 \pm 13.0\%$ decrease in cell viability. It indicated that LEA-mediated SDT had a better anti-proliferative effect on HepG2 cells than artemether-mediated SDT. In addition, the uptake of artemether by tumor cells was increased due to the encapsulation of liposomes. Ultrasound can also induce liposomal drug release by transiently forming a pore-like defect in the liposome membrane through which the drug is released rapidly.[81] To further improve site-specific enrichment of liposomes. Yue *et al.* used liposomes as carriers to co-encapsulate the sonosensitizer hematoporphyrin monomethyl ether (HMME) and immune adjuvants imiquimod (R837) (HMME/R837@Lip) (Fig. 5A). The excellent biocompatibility of the liposomes allows the composite nanosensitizer to be well dispersed in aqueous solution. After systemic administration, HMME/R837@Lip nanosensitizer obtained high tumor accumulation and prolonged tumor retention. Combining anti-PD-L1 not only effectively inhibited primary tumor growth but also significantly prevented simulated distant metastases and lung metastases. The encapsulation of liposomes confers additional functionality to the nanosensitizer. Various combinatorial paradigms can maximize the benefits of anti-cancer therapy and have advantages over the use of single sonosensitizers or anti-cancer drugs.[25]

Traditional liposomes often suffer from premature release and insufficient targeting ability. To further enhance the targeting of sonosensitizers, Qu *et al.* combined sonoactive chlorin e6 (Ce6) and autophagy inhibitor-hydroxychloroquine (HCQ) into angiopep-2 peptide-modified liposomes (designated as ACHL), used to enhance SDT therapy (Fig. 5B). Because the lysosomal drug hydroxychloroquine requires high doses and has serious side effects, which limits its clinical application, and liposome encapsulation can minimize the toxic effects of HCQ, this liposomal nanocarrier has been successfully tested to target drugs to tumors. In addition, nanocarriers functionalized with angiopep-2 is a specific ligand that can target low-density lipoprotein receptor-related protein 1 (LRP1) on various tumors, which is a highly efficient targeted delivery system. ACHL-SDT treatment reduces the toxic side effects of antineoplastic drugs, increases drug targeting, significantly inhibits xenograft tumor growth, and prolongs survival in tumor-bearing mice, leading to improved treatment efficiency.[47] In addition to grafting active targeting molecules, several other elements were introduced to diversify functions and consolidate therapeutic efficiency. Chen *et al.* designed a multifunctional nanosonosensitizer system (FA–MnPs) by encapsulating manganese-protoporphyrin (MnP) into folic acid-liposomes

 

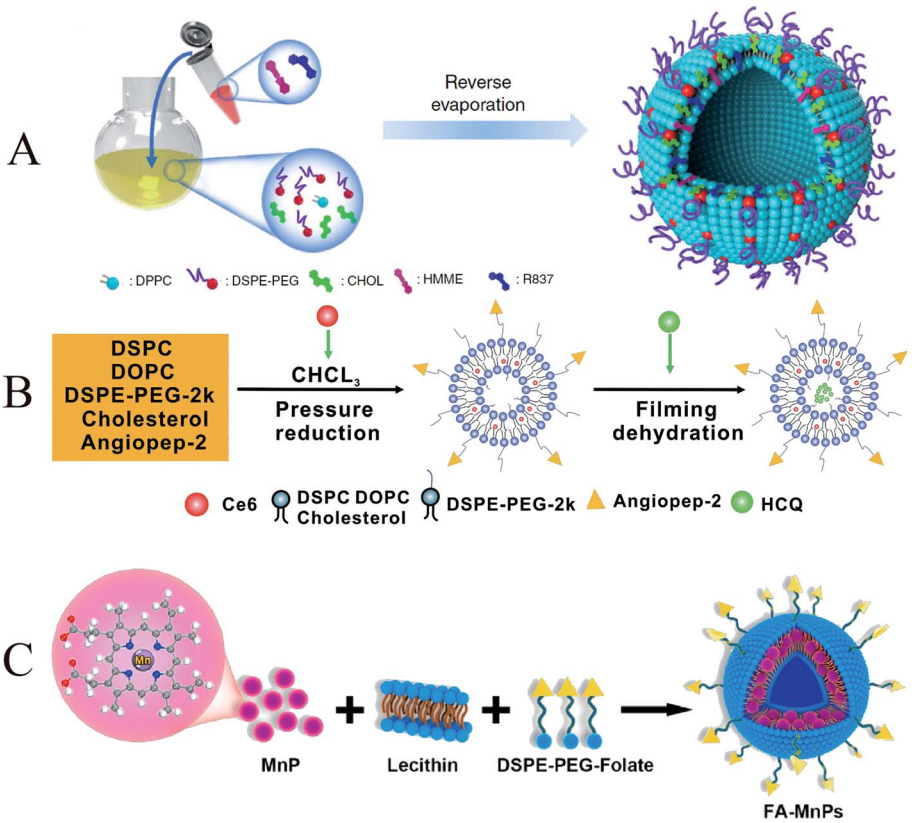


Fig. 5 (A) Schematic illustration of the construction of HMME/R837@Lip nanosonosensitizers and their microstructures; (B) illustration of the simple synthetic process of ACHL liposomes; (C) schematic illustration of FA–MnPs. (A) Reproduced with permission.[24] Copyright 2019, Springer Nature Limited. (B) Reproduced with permission.[46] Copyright 2020, Informa UK Limited. (C) Reproduced with permission.[79] Copyright 2021, Elsevier B.V.

(Fig. 5C). Folate insertion into the liposome bilayer increased the accumulation and transfer of MnP into tumor cells. Metal coordination in MnP enhances US response-ability. FA–MnPs-induced SDT exhibited favorable inhibitory effects on superficial and deep tumors in mice. And it was able to further repolarized immunosuppressive M2 macrophages to anti-tumor M1 macrophages and triggered immunogenic cell death (ICD), thereby triggering anti-tumor immunity and inhibiting tumor growth.[82]

**3.2.3 Inorganic nanomaterials loaded with organic small molecule sonosensitizers.** Inorganic nanoparticles can be developed as efficient delivery carriers for sonosensitizers. Common inorganic sonosensitizer carriers include mesoporous silica, manganese dioxide, semiconductors, metal oxides, *etc.* Mesoporous silica has the advantages of simple preparation, large loading space, good biocompatibility, and accessible surface modification. It can design and prepare different structures, which is beneficial to expand its multifunctionality and is a promising inorganic nanomaterial.[8] Wang *et al.* synthesized holmium-doped hollow silica nanospheres (HHSN–C/PmAb) modified with chlorin e6, carboxy poly(ethylene glycol) silane, and a prostate stem cell antigen (PSCA) monoclonal antibody (Fig. 6A). Due to the cavity structure and Ho doping, HHSN–C/PmAb has high ultrasound (US) imaging contrast capability and excellent high-field magnetic resonance contrast performance. The introduced Ce6 brings sonodynamic performance, and the huge internal cavity can be used to load the bioreductive prodrug tirapazamine TPZ. Under ultrasound, HHSN–C/PmAb produced reactive oxygen species to kill cancer cells, and oxygen consumption during SDT induced hypoxic environment in the tumor to activate co-delivery of TPZ, resulting in a highly efficient synergistic anti-cancer effect.[83] Zhang *et al.* reported a cascade catalytic nanoplatform based on mesoporous $MnO_2$ NPs, in which a sonosensitizer (hematoporphyrin monomethyl ether, HMME) was loaded and the surface was modified with $GO_x$ (Fig. 6B). $GO_x$ can catalyze the oxidation of glucose to $H_2O_2$ and gluconic acid for starvation therapy. HMME acts as a sonosensitizer to generate ROS for SDT. Since both starvation therapy and SDT are dependent on oxygen, $MnO_2$ NPs are crucial to catalyze the oxidation of $H_2O_2$ to generate $O_2$ at the tumor site.[84]

To further improve the stability of nanoparticles under physiological conditions and catalyze the generation of ROS, Liang *et al.* synthesized a novel Pt–CuS Janus composed of hollow semiconductor CuS and noble metal Pt and used it to load a sonosensitizer (tetra-(4-aminophenyl)porphyrin, TAPP) (Fig. 6C). A layer of thermosensitive polymer was wrapped around Janus as a switch to modulate the catalytic ability of Pt and control the release of TAPP. The deposition of Pt enhanced the photothermal performance of CuS and possessed

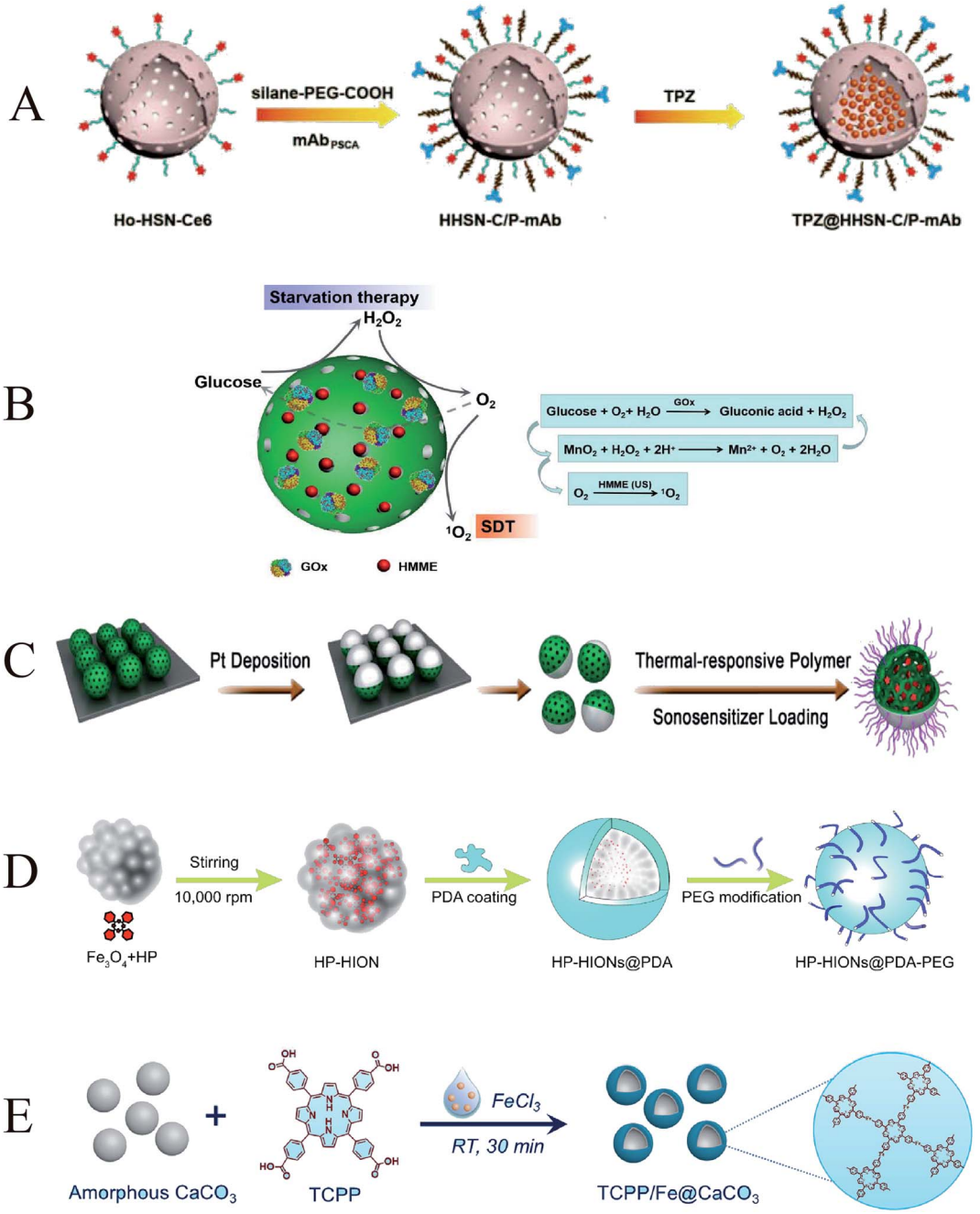


Fig. 6 (A) Schematic illustration of TPZ@HHSN–C/P-mAb; (B) schematic illustration of the cascade catalytic nanoplatform ($GO_x$–$MnO_2$/HMME); (C) schematic illustration of Pt–CuS–P–TAPP; (D) schematic illustration of the synthesis route of HP–HIONs@PDA–PEG; (E) schematic illustration of TCPP/Fe@$CaCO_3$. (A) Reproduced with permission.[80] Copyright 2018, WILEY-VCH. (B) Reproduced with permission.[81] Copyright 2019, Informa UK Limited. (C) Reproduced with permission.[82] Copyright 2019, American Chemical Society. (D) Reproduced with permission.[83] Copyright 2020, Elsevier B.V. (E) Reproduced with permission.[84] Copyright 2020, Elsevier B.V.

nanoenzymatic activity to catalyze the decomposition of endogenously overexpressed $H_2O_2$ to generate $O_2$ that could overcome tumor hypoxia. These properties have significantly improved the anti-tumor therapeutic effect.[85] Not only that, Zhang *et al.* formed a novel magnetic nanosystem by composing hollow iron oxide nanoparticles (HIONs), $Fe_3O_4$, and the sonosensitizer hematoporphyrin (HP) (Fig. 6D). Hollow HIONs can catalyze the decomposition of endogenous overexpressed $H_2O_2$ in tumor tissue to generate $O_2$, enhance SDT-induced ROS production, and promote cell apoptosis. Moreover, the generated ROS can also activate the cleavage of HSP, which further eliminates exercise tolerance and promotes magnetic hyperthermal therapy (MHT) efficacy. The synergistic catalytically enhanced SDT efficiency and MHT effect achieved the most potent tumor suppressor efficacy.[86]

The combination of multiple anti-tumor methods can achieve better anti-tumor effects, which is dependent on the multifunctionality of nanoparticles. Dong *et al.* used $CaCO_3$ nanoparticles as the template, *meso*-tetra-(4-carboxyphenyl) porphine (TCPP) as the sonosensitizer, ferric ion as the metal center, and loaded L-buthionine sulfoximine (BSO), a hollow coordination nanomaterial (BSO–TCPP–Fe@$CaCO_3$) with pH-responsive dissociation was obtained (Fig. 6E). Under the action of BSO–TCPP–Fe@$CaCO_3$, $Ca^{2+}$ was rapidly released, induced mitochondrial damage, and amplified tumor oxidative stress. BSO triggers GSH depletion and TCPP-mediated SDT. Multiple anti-tumor mechanisms are superimposed to obtain better tumor cell killing effect. Tumors in the mice were effectively suppressed after drug administration and ultrasound irradiation.[87]

By encapsulating or connecting organic sonosensitizers with nanomaterials to construct a functionally diverse nanoplatform, the therapeutic efficiency of SDT can be maximized. Therefore, the development of more novel nano-drug delivery systems or new sonosensitizers to promote the efficient application of SDT remains the focus of future research.

### 3.3 Nanomaterials with their sonosensitizers properties

Inorganic sonosensitizers are widely used in SDT and have attracted considerable attention in biomedical applications due to their higher stability and superior physicochemical properties compared to organic sonosensitizers.[7] Many inorganic nanomaterials have acoustic activation capabilities themselves. Herein, we review titanium dioxide nanoparticles, transition metal oxide nanoparticles, noble metal nanoparticles, and carbon-based nanomaterials.

#### 3.3.1 Metal nanomaterials

*3.3.1.1 Titanium dioxide nanoparticles.* $TiO_2$ nanomaterials are the most studied inorganic nano sonosensitizers. Previous studies have shown that under UV light irradiation, the electrons of $TiO_2$ will be transferred from the valence to the conduction band, triggering the generation of a large amount of ROS to achieve PDT, leading to cell death.[88] However, the penetration depth of UV light is limited, and it is not effective for the deep tumors. To overcome this limitation, Shimizu *et al.* found that after replacing UV light with ultrasound, $TiO_2$ can act as a sonosensitizer for SDT, generate ROS, and inhibit tumor cell growth.[89] Subsequently, Harada *et al.* also demonstrated the killing effect of $TiO_2$ on tumor cells under ultrasound.[90]

In recent years, an increasing number of researchers have used $TiO_2$ as a sonosensitizer to mediate SDT. Gao *et al.* reported $TiO_2$-coated Au nanoplates (Au NPL@$TiO_2$) heterostructures (Fig. 7A). Due to the modification of the $TiO_2$ shell on the surface of the 2D Au NPLs, the Au NPL@$TiO_2$ nanostructures are red-shifted to the NIR II region, so the Au NPL@$TiO_2$ nanostructures have a high photothermal conversion efficiency of 42.05% under 1064 nm laser irradiation. Not only that, Au nanoplates (Au NPLs), acting as electron traps, significantly improved the ROS generation of Au NPL@$TiO_2$ nanostructures upon ultrasound (US) activation *via* a sonodynamic process compared to pure shell $TiO_2$ nanoparticles.[91] To further expand the biomedical applications, $TiO_2$ NPs were designed with higher drug loading capacity and higher SDT effectiveness. To further improve the targeted delivery of sonosensitizers, self-assembled inorganic nanoparticles were developed. Feng *et al.* prepared a biomimetic nanoplatform (CCM-HMTNPs/HCQ) based on hollow mesoporous titania nanoparticles (HMTNPs) by autophagy inhibitor (hydroxychloroquine sulfate, HCQ) loading and cancer cell membrane (CCM) coating (Fig. 7B). Due to the biomimetic surface functionalization, CCM-HMTNPs/HCQ nanoparticles could escape from macrophage phagocytosis, actively recognize, and home in on the tumor by homologous targeting ability. Meanwhile, the vascular normalization effect of HCQ alleviated tumor hypoxia and enhanced oxygen-dependent HMTNPs-mediated SDT therapy.[92]

The yield of ROS can promote the tumor-killing efficiency of SDT. Wang *et al.* prepared ultrafine rodlike $TiO_{1+x}$ NRs modified with polyethylene glycol (PEG) (PEG–$TiO_{1+x}$ NRs) (Fig. 7C). The oxygen-deficient structure of $TiO_{1+x}$NR can be used as a charge trap to limit US-triggered electron–hole pair recombination to improve the US-triggered ROS generation efficiency. In addition, PEG–$TiO_{1+x}$ NRs also possess horseradish-peroxidase-like nanozyme activity, which can generate hydroxyl radicals ($^{\bullet}OH$) from endogenous $H_2O_2$ in tumors, thereby enabling chemodynamic therapy (CDT).[93] By modifying $TiO_2$ nanomaterials, it can improve its SDT efficiency and effectively inhibit tumors. Despite some attractive properties, the ROS mass yield of $TiO_2$ NPs is low under US stimulation. To enhance synergistic ultrasound-induced tumor eradication, Cao *et al.* designed a tablet-like $TiO_2$/C nanocomposite with a metal–organic framework (MOF)-derived carbon structure, which exhibits hypoxia-tolerant and stable in response to repeated ultrasound irradiation, making $TiO_2$/C C-mediates the production of large amounts of ROS (Fig. 7D).[94] Similarly, Cai *et al.* successfully synthesized covalent organic framework-titania oxide nanoparticles (COF-$TiO_2$ NPs) using COF as a template (Fig. 7E). Compared with pure $TiO_2$ NPs, the SDT performance of COF-$TiO_2$ nanoparticles is significantly improved due to the narrower band gap.[95]

*3.3.1.2 Transition metal oxide nanoparticles.* In addition to titanium-based nanomaterials, some transition metal oxides such as manganese and iron can also be used for SDT. Gong *et al.* reported an ultra-small anoxic bimetallic oxide $MnWO_x$ nanoparticle ($MnWO_x$–PEG) modified with poly(ethylene glycol) (PEG) (Fig. 8A). The fabricated $MnWO_x$–PEG nanoparticles exhibited a very uniform morphology with an average diameter of $5.74 \pm 1.66$ nm. The oxygen-deficient structure of $MnWO_x$ can provide electron-trapping sites to prevent electron–hole recombination. And $MnWO_x$–PEG has the ability to deplete glutathione, which can further promote the cancer cell-killing effect triggered by SDT.[96] To introduce more functionality, Lin *et al.* designed ultrasound (US) and glutathione (GSH) dual responsive vesicles of Janus Au–MnO nanoparticles (JNPs) coated with PEG and ROS-sensitive polymers (Fig. 8B). Under US irradiation, the vesicles first decomposed into small Janus Au–MnO NPs, and then further decomposed into smaller Au NPs and $Mn^{2+}$. The Au NPs act as a large number of cavitation nucleation sites to enhance

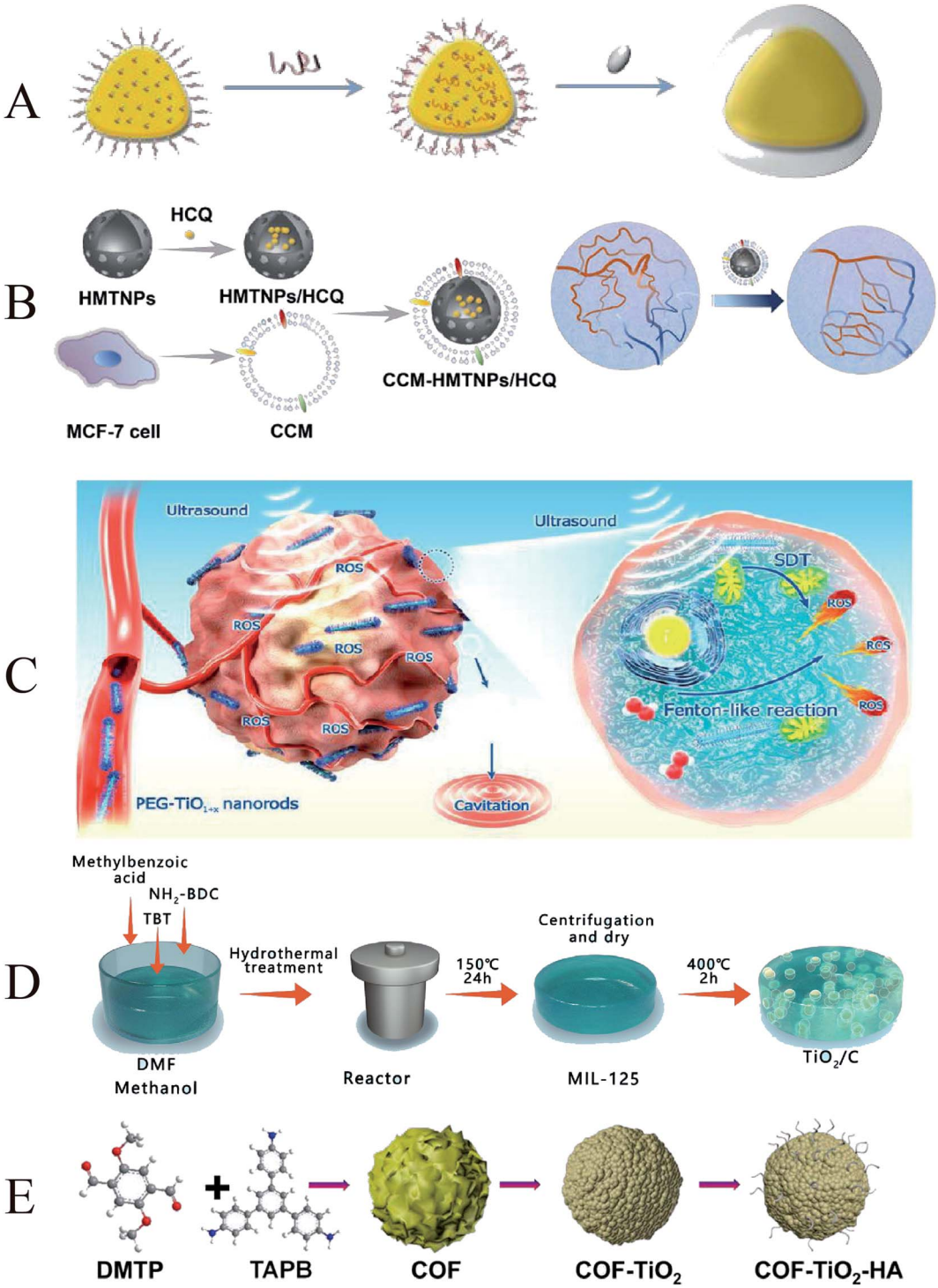


Fig. 7 (A) Schematic illustration of Au NPL@$TiO_2$; (B) schematic illustration of CCM-HMTNPs/HCQ; (C) schematic diagram of ultrafine $TiO_{1+x}$ NRs used for SDT/CDT of cancer; (D) schematic illustration of $TiO_2$/C; (E) schematic illustration of COF-$TiO_2$–HA. (A) Reproduced with permission.[88] Copyright 2019, The Royal Society of Chemistry. (B) Reproduced with permission.[89] Copyright 2019, American Chemical Society. (C) Reproduced with permission.[90] Copyright 2020, American Chemical Society. (D) Reproduced with permission.[91] Copyright 2021, Elsevier B.V. (E) Reproduced with permission.[92] Copyright 2021, American Chemical Society.

the cavitation effect, and the $Mn^{2+}$-induced Fenton reaction enhances the generation of ROS and improves the efficacy of SDT. Due to the released $Mn^{2+}$, this smart nanoplatform also enables dual-modality photoacoustic imaging and T1-MR imaging in the second near-infrared (NIR) window, synergistically suppressing orthotopic liver tumor growth with SDT/CDT.[97] MOF-derived bilayer hollow manganese silicate nanoparticles (DHMS) were prepared by Pan *et al.* (Fig. 8C). In ultrasound and

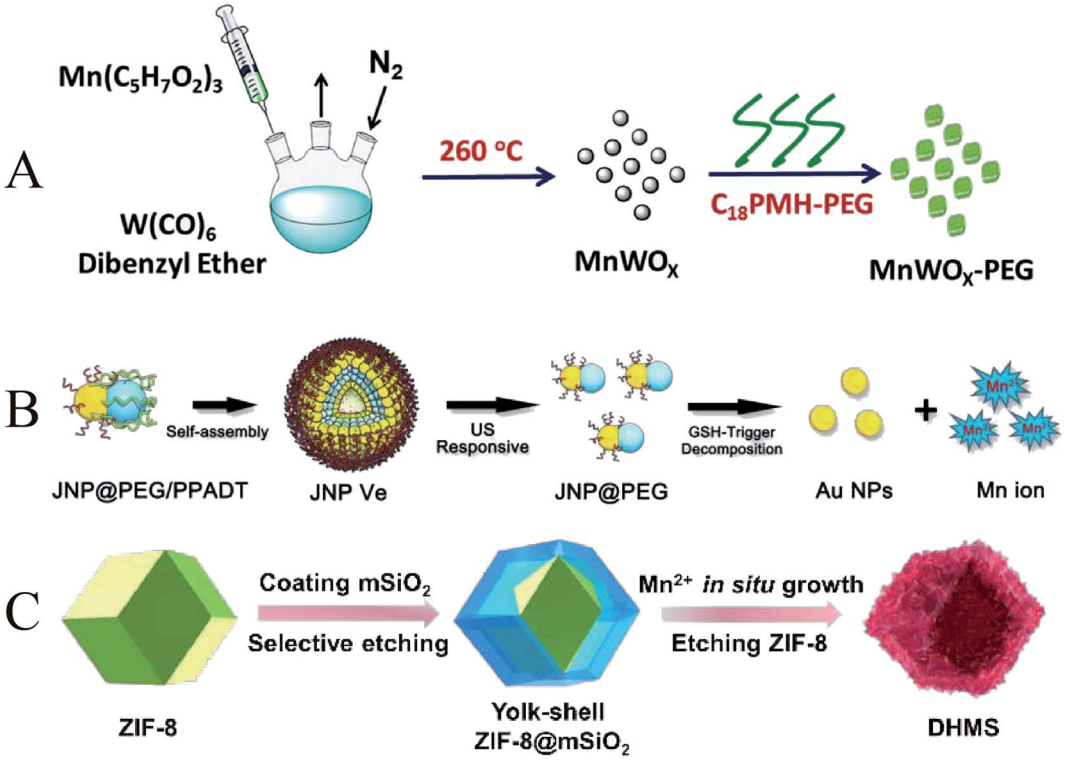


Fig. 8 (A) Schematic illustration of $MnWO_x$; (B) schematic illustration of Janus Au–MnO NPs; (C) schematic illustration of DHMS; (A) reproduced with permission.[93] Copyright 2019, WILEY-VCH. (B) Reproduced with permission.[94] Copyright 2019, WILEY-VCH. (C) Reproduced with permission.[95] Copyright 2020, WILEY-VCH.

magnetic resonance imaging-guided DHMS-mediated SDT, hypoxia in solid tumors was improved, thereby increasing the therapeutic efficiency of SDT.[98]

*3.3.1.3 Noble metal NPs.* Noble metals can be combined with nanomaterials to enhance the efficacy of SDT by preventing electron–hole recombination and increasing the amount of ROS. Wang *et al.* reported for the first time that copper–cysteamine (Cu–Cy) was used for SDT treatment of breast cancer, and the ROS generated by Cu–Cy significantly inhibited the tumor growth of 4T1 cancer cell xenografts under ultrasound irradiation (Fig. 9A).[99] Ouyang *et al.* fabricated two-dimensional (2D) semiconductor-based sonosensitizers (Au@BP nanohybrids), the nanohybrids have excellent stability under ultrasonic irradiation, and the layered BP nanosheets can interact with $O_2$ to generate $^1O_2$ (Fig. 9B).[100] The highly reducing TME produced by glutathione (GSH) is able to protect cells from free radical-induced oxidative damage. ROS production can be promoted by depleting GSH.[101] Zhong *et al.* reported that $PtCu_3$ nanocages can act as sonosensitizers to mediate SDT (Fig. 9C). $PtCu_3$ nanocages can also act as horseradish peroxidase (HRP)-like nanoenzyme, catalyzing the decomposition of $H_2O_2$ into $^{\cdot}OH$ under acidic conditions. In addition, $PtCu_3$ nanocages act as another glutathione peroxidase (GSH-Px) nanoenzyme, which can accelerate the process of GSH depletion in the presence of oxidizing molecules, weaken GSH scavenging of ROS, improve chemodynamic therapy and sonodynamic therapy.[102] Similarly, Lei *et al.* used a high-temperature organic solution method to prepare iron-doped vanadium disulfide nanosheets (Fe–$VS_2$ NSs), which were further modified with polyethylene glycol (PEG) (Fig. 9D). Fe–$VS_2$ NSs imparted good Fenton effect to CDT due to the Fe doping. In addition, multivalent Fe and V elements can effectively deplete glutathione (GSH). The Fenton catalytic performance and strong GSH depleting function make Fe–$VS_2$ NSs a promising sonosensitizer.[103]

**3.3.2 Carbon-based nanomaterials.** Carbon-based nanomaterials, including graphene, carbon nanotubes, and fullerenes, are low-dimensional carbon materials that have attracted much attention in the biomedical field in recent years. Their common property is that the $sp^2$-hybridized carbon atoms are arranged in a hexagonal lattice and have the ability to separate $e^-$ and $h^+$.[104] These unique physical and chemical properties are potentially useful in tumor diagnosis and therapy. To improve the activation efficiency and therapeutic effect of US-mediated SDT, Dai *et al.* report a two-dimensional composite sonosensitizer composed of graphene (GR) and $MnO_x$-functionalized semiconducting $TiO_2$ ($MnO_x$/$TiO_2$–GR) (Fig. 9E). The larger surface area and higher electrical conductivity of the GR nanosheets facilitated the efficient separation of $e^-$ and $h^+$, which significantly enhanced the generation efficiency of ROS. The SDT efficiency is also synergistically improved due to the high photothermal conversion capability of graphene.[105] In addition, Behzadpour *et al.* investigated the effect of polypyrrole-coated multi-walled carbon nanotube composites (PPy@MWCNTs) on melanoma in mice. The results showed

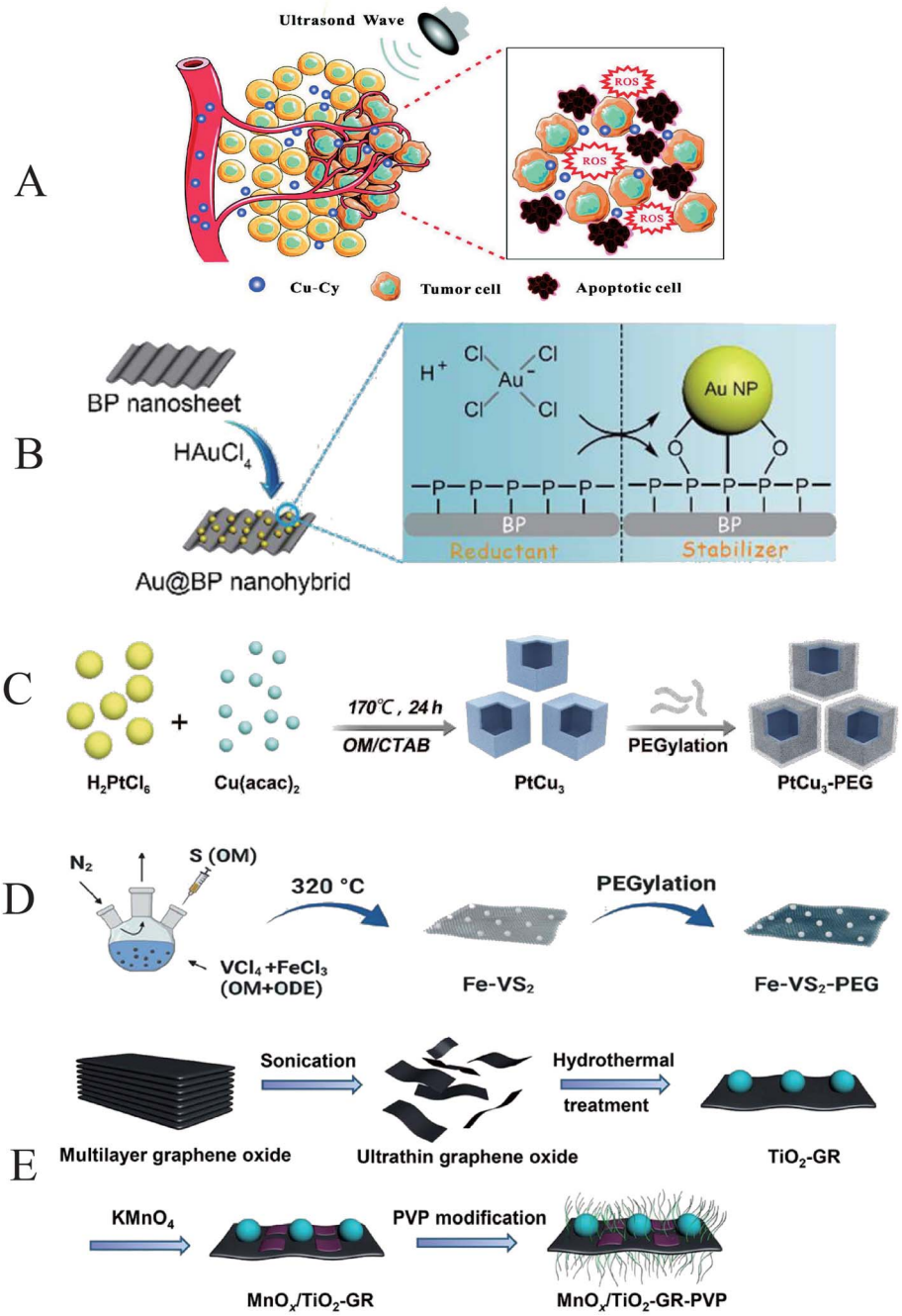


Fig. 9 (A) Schematic illustration of the possible mechanisms of Cu–Cy combined with ultra-sound; (B) schematic illustration of Au@BP nanohybrids; (C) schematic illustration of $PtCu_3$ nanocages; (D) schematic illustration of Fe–$VS_2$ NSs synthesis. (E) Schematic illustration of $MnO_x/TiO_2$–GR–PVP. (A) Reproduced with permission.[96] Copyright 2018, WILEY-VCH. (B) Reproduced with permission.[97] Copyright 2018, The Royal Society of Chemistry. (C) Reproduced with permission.[98] Copyright 2019, WILEY-VCH. (D) Reproduced with permission.[99] Copyright 2020, American Chemical Society. (E) Reproduced with permission.[102] Copyright 2017, American Chemical Society.

that PPy@MWCNTs promoted the killing effect of SDT on tumor cells through thermal effects and ROS.[106]

How to strike a balance between the high sonosensitivity effect and good biosafety of sonosensitizers has always puzzled researchers. Inspired by the potential catalytic activity of graphene quantum dots, Yang *et al.* chose N-doped graphene quantum dots (N-GQDs) as sonosensitizers. Pyrrole N and pyridine N form catalytic centers in the sonochemical processing of N-GQDs. In addition, folate-modified N-GQDs (FA–N-GQDs) marked tumor cells. The results all showed that FA–N-GQDs as a sonosensitizer had a high tumor inhibition efficiency (greater than 90%).[107] However, there are still several aspects that need to be improved for the application of carbon-based nanomaterials in the field of SDT, such as instability and low solubility. Therefore, we need to continue to look for new

materials, introduce new functions, and develop safer and more efficient sonosensitizers.

## 4. Sonodynamic therapy-based combination therapy

Although sonodynamic therapy has shown great potential in tumor treatment, the current therapeutic effect of SDT still cannot meet the therapeutic needs.[108] On the one hand, the biosafety of sonosensitizers limits their clinical applications. On the other hand, due to the heterogeneity and drug resistance of tumor cells, monotherapy is difficult to achieve good efficacy in the treatment of malignant tumors. The combination of SDT with other cancer treatments has shown great potential as a new tumor treatment strategy.[21,109] In this section, we broadly summarize and discuss several SDT-based combination therapy strategies, including chemotherapy, photodynamic therapy (PDT), chemodynamic therapy (CDT), immunotherapy, and photothermal therapy (PTT) (Table 3).

### 4.1 Sonodynamic therapy combined with chemotherapy

Chemotherapy is one of the main methods of tumor treatment. However, the problems of uneven bioavailability and mismatch of pharmacokinetics/circulating half-life in traditional chemotherapeutic drugs limit their development. And long-term use of chemotherapeutic drugs will make the tumor resistant to drug resistance, which will affect the treatment effect and increase the risk of distant metastasis of the tumor.[110] The combination of SDT and chemotherapy can achieve synergistic effects and reduce systemic toxicity. More importantly, SDT has been shown the ability to enhance drug sensitivity of cancer cells by promoting the cellular internalization of chemotherapeutic drugs, activating the mitochondrial-caspase signaling pathway, and downregulating the expression levels of ATP-binding cassette transporters proteins.[111] Therefore, many studies have shifted from chemotherapy alone to combination therapy.

To achieve controlled release delivery of the hydrophobic drug ART at tumor sites, Tang *et al.* developed a pH/GSH/ROS triple-responsive PEG–PPMDT nanoparticles loaded with artemether (ART)/$Fe_3O_4$ (Fig. 10A). Nanoparticles can rapidly release drugs to kill tumour cells under the synergistic effect of acidic endoplasmic pH and high intracellular GSH/ROS levels. Under the action of ultrasound and $Fe^{3+}$, the production of ROS can be increased, which further accelerates the release of drugs. After chemo-sonodynamic therapy, tumors in all nude mice xenografted with human hepatocellular carcinoma (HepG2) shrank significantly, and 40% of tumors were eliminated.[112] Cancer develops an antioxidant defense system that protects itself from persistent oxidative stress by overexpressing catalase, superoxide dismutase, glutathione (GSH), therefore, upregulated GSH in cancer levels is considered to be an important barrier to impairing the efficacy of SDT. Wooram *et al.* reported GSH-depleting carboxymethyl dextran nanocomposites with $TiO_2$ as a sonosensitizer, and $MnO_2$ coat as the GSH-consuming chemosensitizer, and carboxymethyl dextran as the hydrophilic shell (Fig. 10B). When the nanocomposites entered cancer cells, $MnO_2$ was reduced to $Mn^{2+}$ to deplete intracellular GSH, thereby inducing the production of intracellular ROS. This cancer-specific strategy can suppress GSH levels to enhance the efficacy of SDT. Under the irradiation of ultrasound, the nanocomposite generates cytotoxic singlet oxygen in cells, which significantly enhances the cytotoxicity to cancer cells. In addition, the chemical sonodynamic activity of the nanocomposites can also induce apoptosis and necrosis of tumor cells. This synergistic treatment showed excellent anti-tumor efficacy.[113] In another related study, Zhang *et al.* grafted Rh onto the CS backbone to synthesize CS–Rh conjugates, designing a novel CD44 receptor-targeting and redox/ultrasound-responsive oxygen-carrying nanoplatform (Fig. 10C). The nanoplatform

Table 3 Category of combination therapy based on SDT in recent years

| Therapy | Materials | US parameters | Biological model | Ref. |
|---|---|---|---|---|
| SDT-chemo | PEG–PPMDT NPs | 1.0 MHz, 2.0 W $cm^{-2}$, 3 min | HepG2 cells | 112 |
| | $MnO_2$ | 1.0 MHz, 10.0 W $cm^{-2}$, 5 min | SCC7 cells | 113 |
| | CS–Rh–PFC | 1.2 W $cm^{-2}$, 3 min | B16F10 cells | 114 |
| | CEPH | 0.1 W $cm^{-2}$, 1 min | A549, PC-9, H1975 | 116 |
| | Ce6–PTX@IR783 | 1.0 MHz, 1.0 W $cm^{-2}$, 30 s | 4T1 cells | 117 |
| SDT–PDT | GPC3–CUR-MBs | 3.0 MHz, 2.0 W $cm^{-2}$, 5 min | HepG2 cells | 120 |
| | Ce6–P/W NE | 2.1 MHz, 0.25 W $cm^{-2}$, 1 min | PC-3 cells, HeLa cells | 121 |
| | OA–Ce6 | 1.0 MHz, 0.1 W $cm^{-2}$ | PC9, 4T1 cells | 122 |
| SDT–CDT | Fe–$TiO_2$ NDs | 40 kHz, 3 W $cm^{-2}$, 15 min | 4T1 cells | 124 |
| | Pd/H–$TiO_2$ | 1.0 MHz, 1.5 W $cm^{-2}$, 5 min | C6 cells | 125 |
| | $CoFe_2O_4$–PEG | 1.0 MHz, 0.5 W $cm^{-2}$, 3 min | 4T1 cells | 127 |
| | D-MOF(Ti) | 1.0 MHz, 1.0 W $cm^{-2}$, 2 min | 4T1 cells | 128 |
| SDT–immunotherapy | PEG–CDM–aPD-L1/Ce6 | 2.0 MHz, 2.0 W $cm^{-2}$, 5 min | B16-F10 cells | 133 |
| | Zr–TCPP(TPP)/R837@M | 1.0 MHz, 1.0 W $cm^{-2}$, 1 min | 4T1 cells | 134 |
| | $TiO_2$–Ce6–CpG | 1.0 MHz, 1.0 W $cm^{-2}$, 1 min | Hepa1-6 cells | 135 |
| | sPD-1/Ce6 NBs | 1.1 MHz, 1.8 W $cm^{-2}$, 2 min | H22 cells | 136 |
| SDT–PTT | $ZrO_{2-x}$@PEG/cRGD | 1.0 MHz, 0.5 W $cm^{-2}$, 2 min | 4T1 cells | 139 |
| | H–$Ti_3C_2$–PEG NSs | 40 kHz, 3.0 W $cm^{-2}$, 1 min | 4T1 cells | 140 |
| | $Mn^{2+}$–HAS–Ce6–HCM | 0.5 MHz, 1.0 W $cm^{-2}$, 0.1 s | U87 cells | 141 |

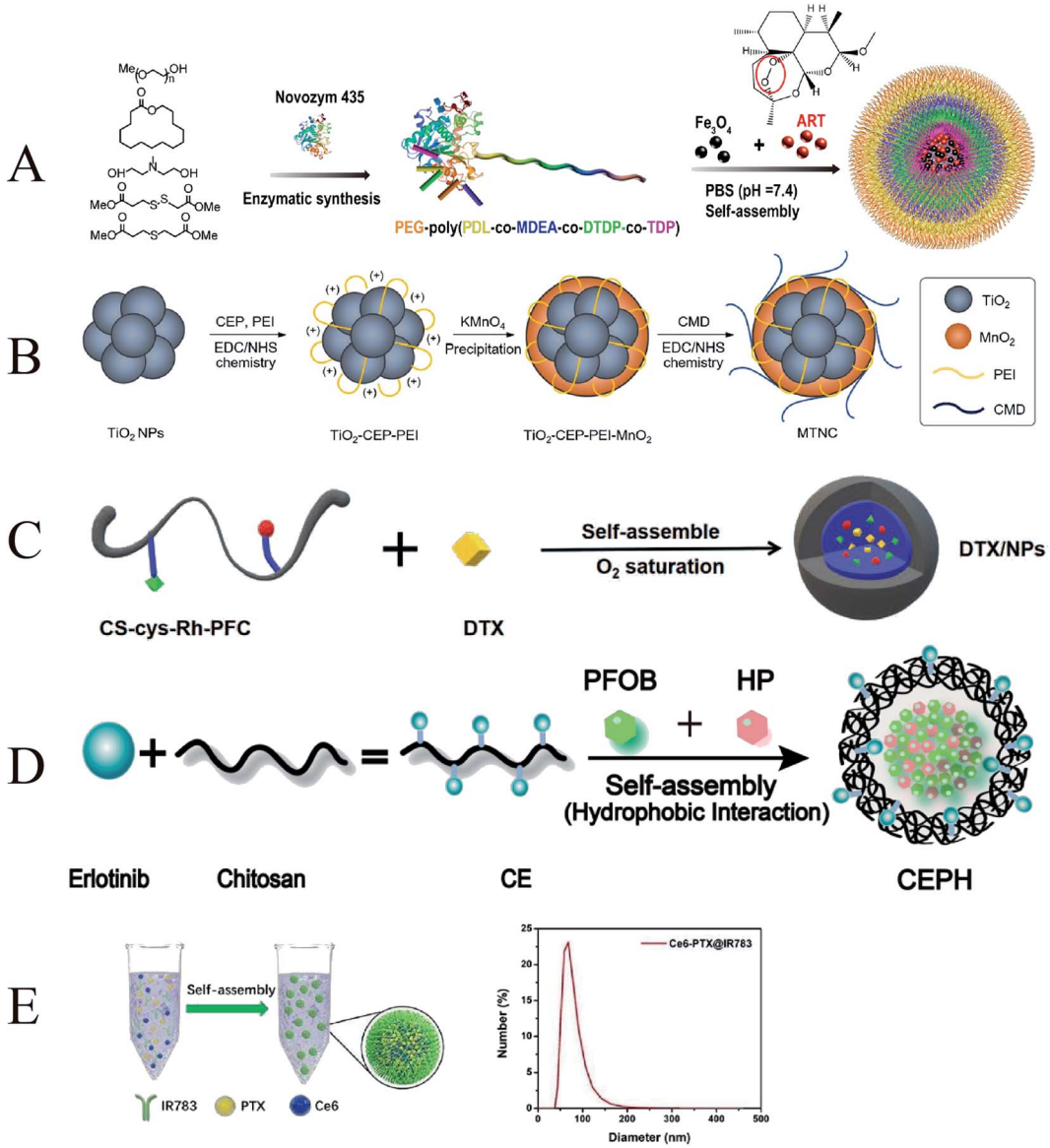


Fig. 10 (A) Schematic illustration of ART/$Fe_3O_4$-loaded PEG–PPMDT NPs; (B) schematic illustration of MTNCs; (C) schematic illustration of DTX-loaded NPs; (D) schematic illustration of CEPH. (E) Schematic illustration of Ce6–PTX@IR783. (A) Reproduced with permission.[109] Copyright 2022, Elsevier B.V. (B) Reproduced with permission.[110] Copyright 2021, Elsevier B.V. (C) Reproduced with permission.[111] Copyright 2021, The Royal Society of Chemistry. (D) Reproduced with permission.[113] Copyright 2021, Elsevier B.V. (E) Reproduced with permission.[114] Copyright 2020, The Royal Society of Chemistry.

also introduced perfluorocarbons (PFCs) to enhance the oxygen-carrying capacity, increasing the oxygen content in B16F10 melanoma cells and improving the efficiency of SDT. Docetaxel (DTX)-loaded NPs induced calreticulin (CRT) exposure after SDT treatment, activated the immune system, and promoted immunogenic cell death. DC maturation after combination chemotherapy–SDT can initiate and direct immune responses.[114]

Targeted molecular therapy (TMT) with epidermal growth factor receptor tyrosine kinase inhibitors (EGFR-TKIs) has been ineffective due to the effects of drug resistance in non-small cell lung cancer.[115] In order to improve the efficiency of anti-cancer drugs, Zhang *et al.* developed a nanoplatform (CEPH) made of erlotinib-modified chitosan loaded with the sonosensitizer hematoporphyrin (HP) and the oxygen storage agent perfluorooctyl bromide (PFOB) (Fig. 10D). CEPH can enhance the TMT/SDT synergistic effect by reducing mitochondrial membrane potential, increasing the efficiency of ROS generation, and downregulating the expression of EGFR, p-EGFR, and HIF-1$\alpha$ proteins. Therefore, CEPH may be a potential nanoplatform to enhance the efficacy of oxygen-dependent SDT and overcome hypoxia-induced TMT resistance to enhance TMT/SDT.[116] Recently, Dong *et al.* used a hydrophilic-hydrophobic self-assembly technique to assemble Ce6 and paclitaxel with IR783 into a nanoscale sonosensitizer Ce6–PTX@IR783

(Fig. 10E). Ce6 can enhance the sonodynamic effect, while PTX acts as a chemotherapeutic, and IR783 is used to increase tumor-specific accumulation and assist in photoacoustic imaging. These facile self-assembly procedures provide an interesting strategy for the efficient utilization of hydrophobic drugs while reducing the biosafety issues associated with the reintroduction of nanocarriers, providing new ideas and prospects for large-scale production and further clinical translation.[117] The development of combined chemotherapy–SDT as a sonodynamic combined treatment mode has been continuously strengthened, and the synergistic treatment effect has been greatly improved. Overall, nanosystems that optimize tumor enrichment, accomplish drug response-specific release, and minimize tumor hypoxia will be critical components of future therapeutic modalities' clinical translation.

### 4.2 Sonodynamic therapy combined with photodynamic therapy (PDT)

The widespread application of PDT is hindered by the low penetration of light into tissue.[118] Compared to PDT, ultrasound in SDT can easily penetrate deep tissue layers, making up for a major limitation of PDT. Meanwhile, most of the sonosensitizers are derived from photosensitizers, which allows these sensitizers to be activated by both US and light irradiation.[119] Therefore, the combination of SDT and PDT was able to generate more ROS, which would increase anti-tumor efficacy. Over the past few years, such combination strategies have proliferated and a large number of encouraging results have been reported.

Ultrasonic and laser activation of the same sensitizer enables sonochemical and photochemical effects. Zhu *et al.* investigated glypican-3-targeted, curcumin-loaded microvesicles (GPC3–CUR-MBs) for SPDT inhibition of hepatoma cells (Fig. 11A). GPC3–CUR-MBs have excellent specific targeting to HepG2 cells. And the inhibitory effect of SPDT on liver cancer was significantly better than that of traditional SDT and PDT.[120] Due to the high 3D precision of photoexcitation, the deep penetration of ultrasound, and the prospect of efficient generation of ROS promoted by oxygen delivery. Similarly, Hong *et al.* also developed a multifunctional nanoformulation, chlorin e6–perfluoropolyether water nanoemulsion (Ce6–P/W NE), for combined SDT and PDT treatment of cancer (Fig. 11B).[121]

With the increasing understanding of PTT by researchers, Zheng *et al.* used the hydrophobic anti-tumor drug oleanolic acid (OA) and the photosensitizer chlorin e6 (Ce6) to form a carrier-free nanosensitizer OC by self-assembly technology (Fig. 11C). OC has an average particle size of about 100 nm and has excellent photostability. It exhibited a clear synergistic inhibitory effect on PC9 and 4T1 cells under light and US irradiation, and the $IC_{50}$ value was significantly reduced. The results of experiments showed that OC had a significant inhibitory effect on the tumor of 4T1 mammary tumor-bearing mice. *In vivo* and *in vitro* studies

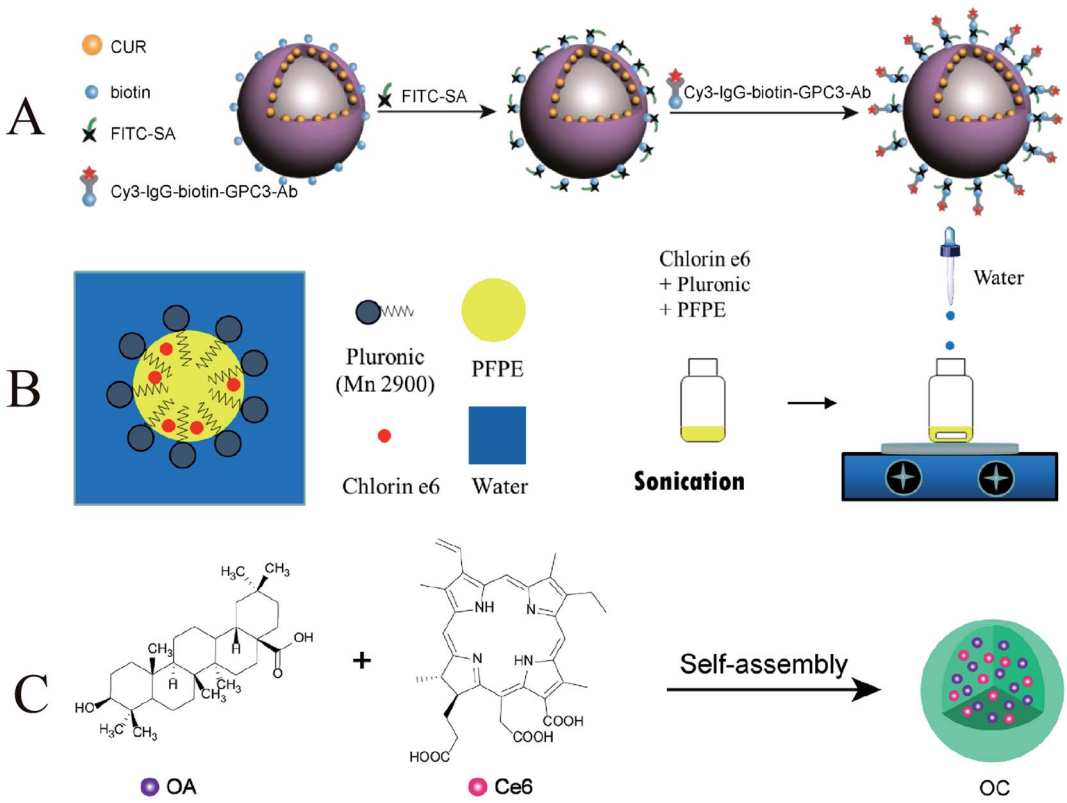


Fig. 11 (A) Schematic illustration of GPC3-Ab and CUR-MB binding *via* SA and biotin; (B) schematic illustration of Ce6–P/W NE; (C) schematic illustration of OC; (A) reproduced with permission.[117] Copyright 2022, Elsevier B.V. (B) Reproduced with permission.[118] Copyright 2020, MDPI. (C) Reproduced with permission.[119] Copyright 2021, Elsevier B.V.

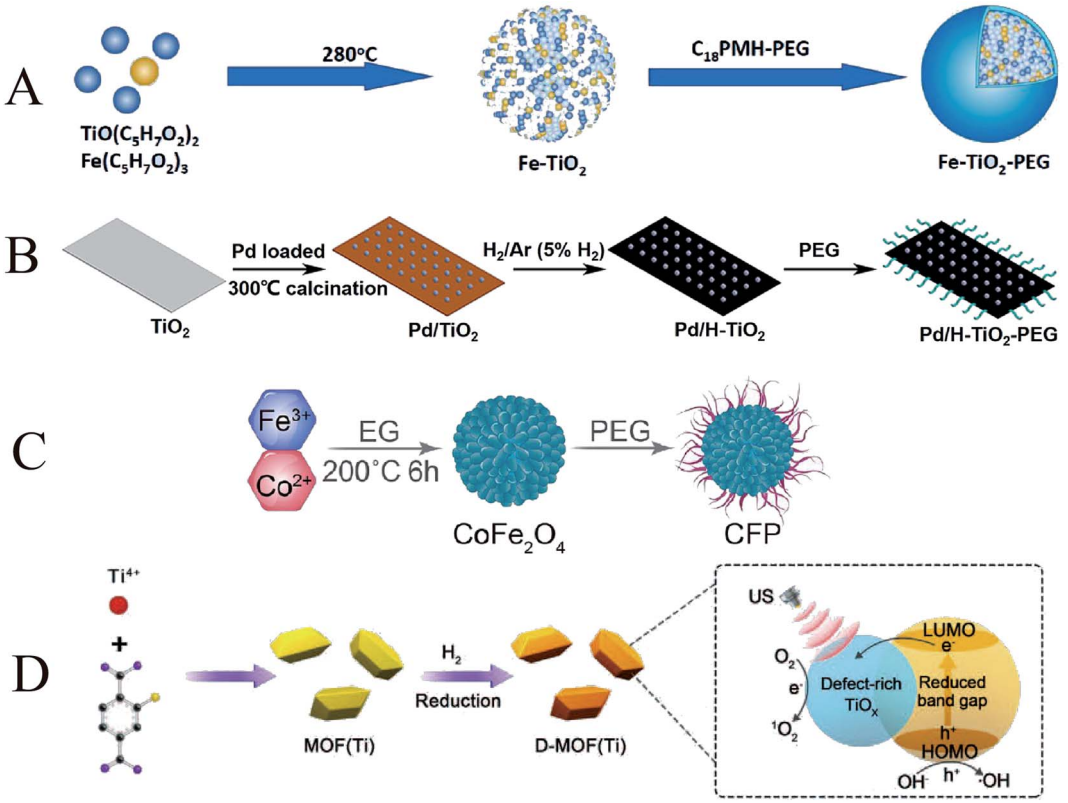


Fig. 12 (A) Schematic illustration of Fe–$TiO_2$ NDs; (B) schematic illustration of Pd/H–$TiO_2$–PEG; (C) schematic illustration of CPF; (D) schematic illustration of D-MOF(Ti). (A) Reproduced with permission.[121] Copyright 2021, American Chemical Society. (B) Reproduced with permission.[123] Copyright 2022, BioMed Central Ltd. (C) Reproduced with permission.[124] Copyright 2021, American Chemical Society. (D) Reproduced with permission.[125] Copyright 2021, WILEY-VCH.

suggest that OC may be a promising therapeutic agent for cancer treatment with synergistic chemo/sono-photodynamic therapy. Since some nano-sonosensitizers also have excellent photosensitization effects, they exert anti-tumor effects through different mechanisms to achieve combined therapy.[122] Furthermore, due to limited tissue penetration of the light source employed, therapy of deep tumors may remain unsatisfactory. This combination will be a potential treatment for the excision of deeper cancers when light delivery technology develops, such as built-in optical fibers or wireless photonics.

### 4.3 Sonodynamic therapy combined with chemodynamic therapy (CDT)

Oxygen uptake due to abnormal tumor vasculature and rapid proliferation of cancer cells can lead to hypoxia in solid tumors.[123] To address this issue, researchers have tried various strategies to achieve hypoxia and enhance the effect of SDT therapy to improve the hypoxic state of the tumor. Bai *et al.* synthesized ultra-small iron-doped titania nanodots (Fe–$TiO_2$ NDs) by thermal decomposition (Fig. 12A). The modification of polyethylene glycol (PEG) enables Fe–$TiO_2$ NDs to exhibit good physiological stability and biocompatibility. The doping of Fe not only promoted the occurrence of Fenton reaction but also promoted the generation of $O_2$ from endogenous $H_2O_2$ in the tumor. Due to the combination of CDT and SDT, Fe–$TiO_2$ NDs exhibited better *in vivo* anti-tumor effects than conventional $TiO_2$ nanoparticles.[124] Compared with native enzymes, nanozymes are considered as promising theranostic adjuvants due to their tunable enzymatic activity, higher stability, and lower production cost.[125] Similarly, Qiao *et al.* fabricated a Pd/H–$TiO_2$ nanosheet (NSs) (Fig. 12B). Unlike conventional $TiO_2$ nanoparticles, Pd/H–$TiO_2$ nanosheets (NSs) can also be used as Fenton-like agents by promoting hydrogen oxide is converted to ·OH for chemodynamic therapy. The Pd component has catalase-like activity and generates oxygen to improve hypoxia.[126]

Following a similar design, Fu *et al.* synthesized pegylated $CoFe_2O_4$ nanoflowers (CFPs) with multiple enzymatic activities by a solvothermal method (Fig. 12C). CFP itself is a sonosensitizer based on ultrasound-triggered electron ($e^-$)/hole ($h^+$) pair separation from the energy band rapidly and efficiently, capable of triggering SDT. In addition, CFP can also generate a Fenton reaction to generate ·OH for CDT. CFP with catalase-like activity can react with endogenous $H_2O_2$ in tumors to generate $O_2$ and relieve tumor hypoxia.[127] MOF materials with photocatalytic properties may have great potential for SDT applications. Liang *et al.* constructed a defect-rich titanium-based metal–organic framework (MOF) (D-MOF(Ti)) (Fig. 12D). Compared with ordinary $TiO_2$, this organic framework can improve the US-triggered electron–hole separation with higher ROS yield. At

the same time, the presence of $Ti^{3+}$ makes D-MOF(Ti) also show a high level of Fenton-like activity, which can be used for chemodynamic therapy. The Fenton reaction was also enhanced by SDT under US irradiation. This work serves as an example of a novel titanium-based material with excellent combined SDT and CDT performance.[128] In conclusion, CDT's dependence on endogenous ROS to kill cancer cells makes it play an important role in cancer therapy. However, the therapeutic effect of CDT is limited due to the limited endogenous reaction substrates in tumors. When CDT is combined with SDT, enhancing the efficiency of ROS generation and promoting the diffusion of nanoparticles to the deep sites of the tumor can significantly improve the therapeutic effect on the tumor.[129] Therefore, it is important to develop nanomaterials with high tumor specificity that bind CDT and SDT and modulate the tumor microenvironment.

### 4.4 Sonodynamic therapy combined with immunotherapy

In recent decades, researchers have developed various types of cancer immunotherapies to enhance the immune system's response to tumors. Tumor cell fragments induced by SDT-mediated apoptotic or necrotic cancer cells can also act as antigens to elicit host anti-tumor immunity, but the anti-tumor immune response elicited by SDT is not sufficient to effectively inhibit tumor growth and metastasis.[130,131] Therefore, developing alternative strategies to enhance immune responses based on SDT is of great clinical interest. SDT has been reported to induce acute inflammation and promote lymphocyte infiltration of tumors, thereby triggering anti-tumor immunity. However, the anti-cancer immunity triggered by SDT is still weak and cannot effectively inhibit tumor growth and recurrence. Therefore, SDT may need to act synergistically with other immunotherapeutic agents to trigger potent anticancer immunity and long-term immune memory.[132] Huang *et al.* developed a lipid (LP)-based micellar nanocarrier that encapsulated the sonosensitizer chlorin e6 (Ce6) and conjugated an anti-PD-L1 antibody (aPD-L1) to the middle layer (Fig. 13A). This nanocarrier enables tumor-targeted delivery to activate anti-tumor immunity while reducing immune-related adverse effects (irAEs). The combination of SDT and aPD-L1 immunotherapy effectively promoted the activation of cytotoxic T cells and improved the immune infiltration of tumors, resulting in strong anti-tumor immunity and long-term immune memory. This tumor-targeted co-delivery strategy of immune checkpoint

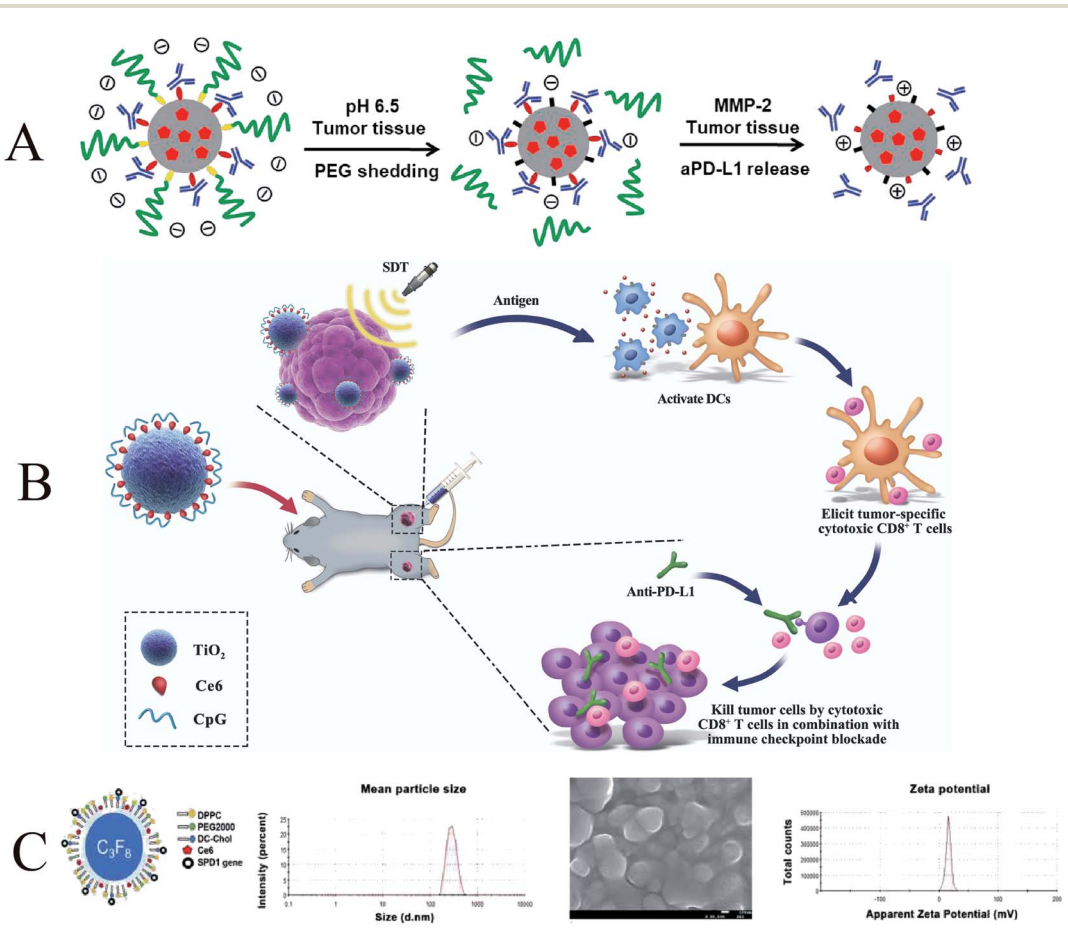


Fig. 13 (A) Schematic illustration of P-aPD-L1/C; (B) schematic illustration of antitumor immunity induced by combined noninvasive SDT with nanosonosensitizers and checkpoint blockade for effective cancer immunotherapy; (C) schematic illustration of sPD-1/Ce6-NBs. (A) Reproduced with permission.[129] Copyright 2020, Elsevier B.V. (B) Reproduced with permission.[131] Copyright 2021, Dove Press Ltd. (C) Reproduced with permission.[132] Copyright 2021, Dove Press Ltd.

inhibitors and SDT drugs effectively inhibited melanoma growth and postoperative recurrence.[133]

SDT-induced *in situ* release of primary tumor TAA can trigger vaccine-like activity, especially in combination with immune adjuvants, by inducing DC maturation and associated cytokine secretion and tumor-killing to trigger potent immunity. Luo *et al.* synthesized TPP-conjugated porphyrin-based nMOFs (Zr–TCPP(TPP)/R837@M) modified with 4T1 cell membrane. When TCPP(TPP)/R837@M was used concomitantly with the R837 immune adjuvant, it could induce DC maturation and associated cytokine secretion and tumor-killing to elicit an immune response. When it was combined with anti-CTLA-4 ICB therapy, increased $CD8^+$ T cell infiltration resulted in stronger antitumor immunity.[134] In the context of another immunotherapy, Lin *et al.* have developed an effective tumor treatment strategy by using cascaded immunosonodynamic therapy (immuno-SDT) (Fig. 13B). The sonosensitizer chlorin e6 (Ce6) and the immunoadjuvant CpG oligonucleotide (CpG ODN) were loaded on titanium dioxide ($TiO_2$) to construct a multifunctional nanosonosensitizer ($TiO_2$–Ce6–CpG). Nano sonosensitizers ($TiO_2$–Ce6–CpG) can not only effectively inhibit tumor growth, but also stimulate the immune system to activate adaptive immune responses. Enhancement of immune responses using $TiO_2$–Ce6 to enhance SDT and immune adjuvant CpG. Cascade immune SDT further combined with aPD-L1 checkpoint blockade therapy synergistically inhibits not only primary tumor growth but also unirradiated pre-existing distant tumors by inducing a strong tumor-specific immune response.[135] To combine soluble programmed cell death protein 1 (sPD-1)-mediated immune checkpoint therapy and chlorin e6 (Ce6)-assisted

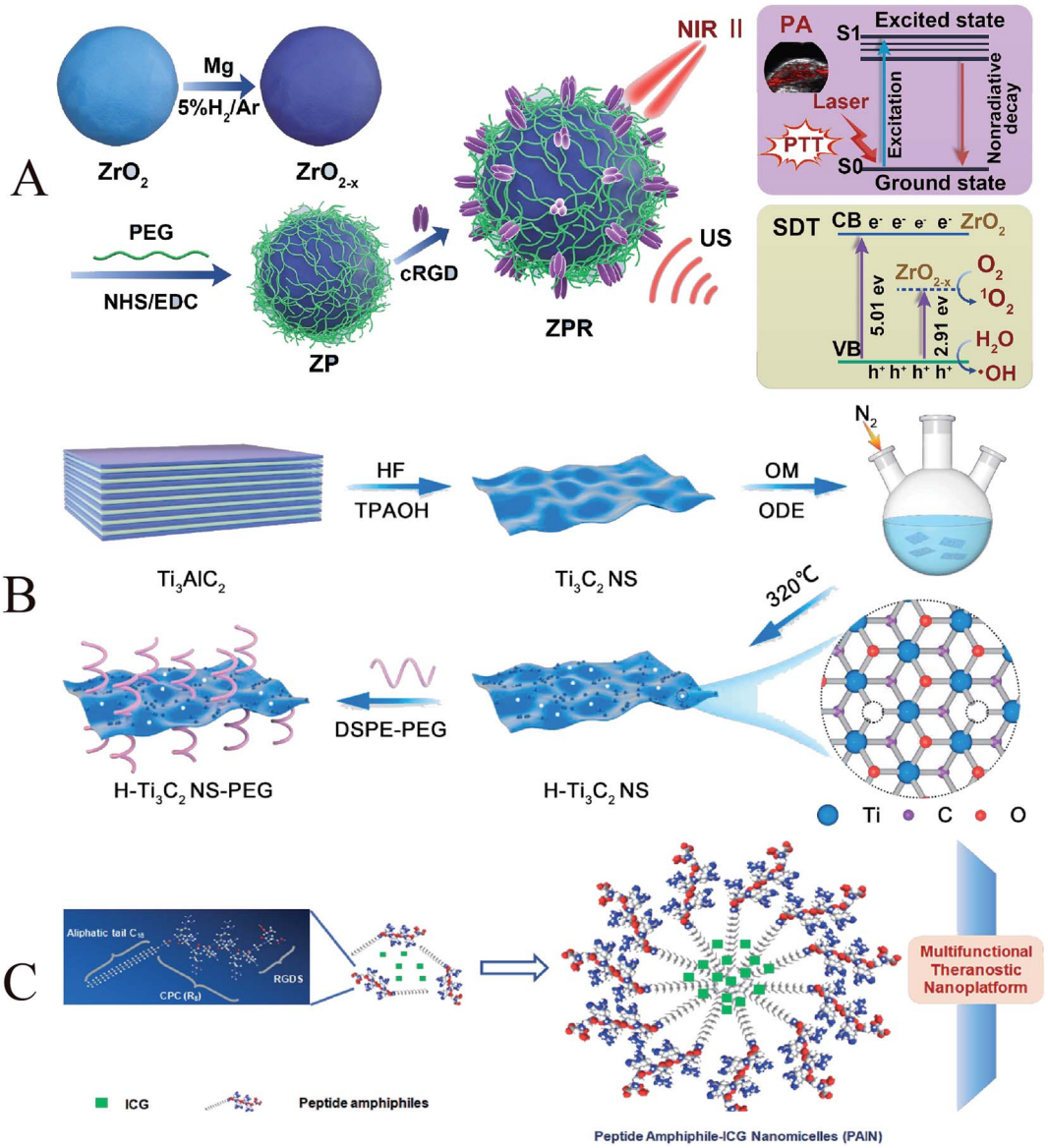


Fig. 14 (A) Schematic illustration of ZPR NPs; (B) schematic illustration of HH-$Ti_3C_2$ nanosheets; (C) schematic illustration of HCM NAs; (A) reproduced with permission.[135] Copyright 2021, Elsevier B.V. (B) Reproduced with permission.[136] Copyright 2021, Elsevier B.V. (C) Reproduced with permission.[137] Copyright 2019, Elsevier B.V.

SDT, Tan *et al.* encapsulated sPD-1 and Ce6 with nanobubbles (NB) (Fig. 13C). NBs enhance the tumor-targeted accumulation and induce ultrasound targeting by targeted delivery of sPD-1 and Ce6. When tumor cells are transfected with sPD-1, the expression of programmed death ligand 1 (PD-L1) in tumor cells can be down-regulated, blocking the PD-1/PD-L1 signaling pathway, and promoting T cell-mediated tumor suppression. This new therapeutic strategy may offer promising new solutions for treating deeper tumors.[136]

Immunotherapy has been widely favoured by researchers in recent years. Combined with ultrasound, the ability to activate the immune system to inhibit tumor metastasis and recurrence provides a broad prospect for the clinical treatment of tumors. However, the combination of SDT and immunotherapy is still at an early stage. Due to the complex immune mechanism, the synergistic effect of the two is still unclear. Therefore, high requirements are also placed on designing such synergistic therapeutic vectors.

### 4.5 Sonodynamic therapy combined with photothermal therapy (PTT)

Photothermal therapy is adjuvant therapy for tumor treatment, which raises the local temperature of the tumor to 40–43 °C, but does not increase the temperature of surrounding normal tissues.[137] Photothermal therapy can alter the blood supply and oxygenation of tumor cells, alleviate tumor hypoxia and promote SDT-mediated ROS production, ultimately resulting in an effective synergistic therapeutic effect.[138] Jiao *et al.* synthesized functionalized nanoplatform $ZrO_{2-x}$@PEG/cRGD (abbreviated as ZPR) by modifying oxygen-deficient zirconia nanoparticles with PEG and cRGD (Fig. 14A). ZPR nanoparticles exhibit strong absorbance in the wavelength range of 900–1100 nm, making the photothermal conversion efficiency of ZPR nanoparticles as high as 45.8%. After applying external stimulation with NIR-II/US, ICD was effectively triggered, synergizing with SDT/PTT, to completely eradicate tumors by promoting anti-tumor immunogenicity.[139]

Due to the limited endogenous $H_2O_2$ and weak $O_2$ transport efficiency to the tumor site, the photothermal effect to improve the tumor hypoxic microenvironment is the simplest and most convenient method. Li *et al.* developed $Ti_3C_2$ MXene nanosheets ($Ti_3C_2$ NSs) as good sonosensitizers through chemical exfoliation and high-temperature treatment (Fig. 14B). Under high temperature and ultrasonic irradiation, electrons ($e^-$) and holes ($h^+$) can be separated faster due to the increased oxidation degree, and abundant oxygen defects can also prevent the recombination of $e^-$–$h^+$. Through these mechanisms, the sonodynamic efficiency is increased by about 3.7 times compared to the $Ti_3C_2$ NSs without high-temperature treatment. Photothermal therapy (PTT) can enhance SDT through *in vivo* and *in vitro* experiments.[140] Similarly, Liu *et al.* treated glioblastoma (GBM) with heat treatment and sonodynamic therapy. They prepared manganese ion ($Mn^{2+}$)-chelated human serum albumin (HSA)–chlorin e6 (Ce6) nanoassemblies (HCM NAs) as targeted nanosonosensitizers. Both *in vitro* cellular and *in vivo* therapeutic results demonstrate the synergistic enhancement of FUS irradiation by these nanocomponents (Fig. 14C). More importantly, treatment in the nanocomponent + FUS (42 °C) group completely inhibited tumor progression in a subcutaneous glioma mouse model. This two-in-one therapeutic strategy provides a new perspective for cancer treatment and shows excellent potential for clinical application.[141]

Based on the above discussion, we believe there is great potential in exploring the combination of SDT adjuvant with other treatment modalities for clinical translation. However, the combination of SDT with immunotherapy is still in its early stages, and the synergy between the two is unclear due to the complex immune mechanisms. Excessive immune activation also has the potential to induce autoimmune reactions, which may induce autoimmune diseases. Therefore, it is necessary to explore in depth the therapeutic mechanisms and optimal regimens of SDT combined with immunotherapy.

## 5. Summary and outlook

There is no doubt that SDT has shown desirable results in cancer treatment and drug delivery applications as a non-invasive, highly efficacious, minimal lateral damage treatment strategy. Despite the many advantages of SDT, the clinical translation of SDT is limited by the nature of the sonosensitizer, the efficacy of which is closely related to its efficacy.

Although great progress has been made in the development of sonosensitizers, there are still many issues that need to be addressed before entering the clinical application phase. (1) The mechanism of SDT is still unclear, and a more in-depth understanding of the mechanism of SDT, mainly including ultrasonic cavitation, generation of ROS, and ultrasound-induced apoptosis, should be provided in the future. Further understanding of the mechanism of SDT can help design therapeutic diagnostic nanomaterials with better targeting efficiency and therapeutic effect for its unique mechanism. (2) The composition and structure of multi-component nanosonosensitizers need to be carefully designed and precisely constructed, and interdisciplinary cooperation among biology, materials, clinical and imaging should be widely carried out to explore novel sonosensitizers with high efficacy by optimizing the structure and acoustic capability. (3) The toxicity and biocompatibility of nanosonosensitizers limit their further clinical applications. Numerous experiments are needed to verify their long-term toxic effects. Only when their biosafety is fully established will these nanomaterial-based sonosensitizers be able to enter the clinical trial stage. (4) The ultrasound parameters and the efficacy of SDT are closely related. Over time, there has been a lack of consistency in the ultrasound parameters used in different studies. Therefore, there is a need to develop appropriate standard operating procedures and design and develop special equipment and instruments for SDT. The selection of appropriate ultrasound parameters, such as frequency, intensity, treatment duration, and mechanical index, can improve the therapeutic efficacy of SDT. This requires extensive in-depth and comprehensive research.

The efficacy of SDT is highly dependent on the properties of the sonosensitizer. Improving the efficiency of sonosensitizer

can focus on overcoming biological barriers, improving tumor-targeted and intratumoral delivery, providing controlled release characteristics of the stimulus response, stimulating antitumor immunity, and increasing oxygen supply.

Due to the complexity and diversity of many tumors, SDT monotherapy may not be sufficient to combat cancer effectively and consistently. As a result, combination therapies have expanded treatment options and become popular. SDT-based combination therapies have been shown to significantly improve treatment outcomes by intelligently integrating SDT with other therapeutic modalities to modulate multiple signaling pathways. Therefore, we believe that nanomaterials-assisted combination SDT therapies have great potential for clinical translation.

Future research should focus on these aspects: (1) optimizing the composition and structure of nanosonosensitizers to develop nanomaterials with better targeting efficiency and therapeutic effects; (2) further improving the biocompatibility and effectiveness of nanosonosensitizers; (3) increasing the research on SDT combined with other therapies to facilitate their translation to the clinic. In summary, SDT-based tumor therapy is still in its infancy. There is a wide space for innovative research on the interdisciplinary development of nanotechnology combined with medicine, which still needs our continuous exploration.

## Conflicts of interest

The authors declare no conflict of interest.

## Acknowledgements

This work was financially supported by Hunan Health Commission (Grant No. 20201906), Hunan Science and Technology Department (Grant No. 2018sk51705), Hengyang Science and Technology Department (Grant No. 2021115).

## Notes and references

1 R. L. Siegel, K. D. Miller, H. E. Fuchs and A. Jemal, *Ca-Cancer J. Clin.*, 2021, **71**, 7–33.
2 H. G. Welch, B. S. Kramer and W. C. Black, *N. Engl. J. Med.*, 2019, **381**, 1378–1386.
3 N. Yumita, R. Nishigaki, K. Umemura and S. i. Umemura, *Jpn. J. Cancer Res.*, 1989, **80**, 219–222.
4 T. J. Mason, *Ultrason. Sonochem.*, 2011, **18**, 847–852.
5 G. J. Lu, A. Farhadi, J. O. Szablowski, A. Lee-Gosselin, S. R. Barnes, A. Lakshmanan, R. W. Bourdeau and M. G. Shapiro, *Nat. Mater.*, 2018, **17**, 456–463.
6 A. P. McHale, J. F. Callan, N. Nomikou, C. Fowley and B. Callan, *Therapeutic Ultrasound*, 2016, pp. 429–450.
7 H. Chen, X. Zhou, Y. Gao, B. Zheng, F. Tang and J. Huang, *Drug Discovery Today*, 2014, **19**, 502–509.
8 G. Canavese, A. Ancona, L. Racca, M. Canta, B. Dumontel, F. Barbaresco, T. Limongi and V. Cauda, *Chem. Eng. J.*, 2018, **340**, 155–172.
9 S. Kwon, H. Ko, D. G. You, K. Kataoka and J. H. Park, *Acc. Chem. Res.*, 2019, **52**, 1771–1782.
10 H. Xu, X. Zhang, R. Han, P. Yang, H. Ma, Y. Song, Z. Lu, W. Yin, X. Wu and H. Wang, *RSC Adv.*, 2016, **6**, 50697–50705.
11 M. Trendowski, *Cancer Metastasis Rev.*, 2014, **33**, 143–160.
12 E. Li, Y. Sun, G. Lv, Y. Li, Z. Zhang, Z. Hu and W. Cao, *Int. J. Biochem. Cell Biol.*, 2019, **113**, 104–114.
13 S. Dai, C. Xu, Y. Tian, W. Cheng and B. Li, *Oncol. Lett.*, 2014, **8**, 1675–1681.
14 L. Zhao, R. Zheng, L. Liu, X. Chen, R. Guan, N. Yang, A. Chen, X. Yu, H. Cheng and S. Li, *Biomaterials*, 2021, **275**, 120970.
15 Y. Ma, Y. Zhang, X. Li, Y. Zhao, M. Li, W. Jiang, X. Tang, J. Dou, L. Lu and F. Wang, *ACS Nano*, 2019, **13**, 11967–11980.
16 L. Jin, S. Shen, Y. Huang, D. Li and X. Yang, *Biomaterials*, 2021, **268**, 120582.
17 Q. Chen, J. Chen, Z. Yang, J. Xu, L. Xu, C. Liang, X. Han and Z. Liu, *Adv. Mater.*, 2019, **31**, 1802228.
18 L.-S. Lin, J.-F. Wang, J. Song, Y. Liu, G. Zhu, Y. Dai, Z. Shen, R. Tian, J. Song and Z. Wang, *Theranostics*, 2019, **9**, 7200.
19 X. Wang, X. Zhong, F. Gong, Y. Chao and L. Cheng, *Mater. Horiz.*, 2020, **7**, 2028–2046.
20 Y. Chen, B. Yin, Z. Liu, H. Wang, Z. Fu, X. Ji, W. Tang, D. Ni and W. Peng, *Nano Res.*, 2022, 1–8.
21 X. Pan, H. Wang, S. Wang, X. Sun, L. Wang, W. Wang, H. Shen and H. Liu, *Sci. China: Life Sci.*, 2018, **61**, 415–426.
22 N. Rabiee, M. T. Yaraki, S. M. Garakani, S. M. Garakani, S. Ahmadi, A. Lajevardi, M. Bagherzadeh, M. Rabiee, L. Tayebi and M. Tahriri, *Biomaterials*, 2020, **232**, 119707.
23 Z. Wang, C. Liu, Y. Zhao, M. Hu, D. Ma, P. Zhang, Y. Xue and X. Li, *Chem. Eng. J.*, 2019, **356**, 811–818.
24 S. Malekmohammadi, H. Hadadzadeh, S. Rezakhani and Z. Amirghofran, *ACS Biomater. Sci. Eng.*, 2019, **5**, 4405–4415.
25 W. Yue, L. Chen, L. Yu, B. Zhou, H. Yin, W. Ren, C. Liu, L. Guo, Y. Zhang and L. Sun, *Nat. Commun.*, 2019, **10**, 1–15.
26 A. Sazgarnia, A. Shanei, A. R. Taheri, N. T. Meibodi, H. Eshghi, N. Attaran and M. M. Shanei, *J. Ultrasound Med.*, 2013, **32**, 475–483.
27 S. Mitragotri, *Nat. Rev. Drug Discov.*, 2005, **4**, 255–260.
28 Q. Wan, C. Zou, D. Hu, J. Zhou, M. Chen, C. Tie, Y. Qiao, F. Yan, C. Cheng and Z. Sheng, *Biomater. Sci.*, 2019, **7**, 3007–3015.
29 S.-T. Kang, J.-L. Lin, C.-H. Wang, Y.-C. Chang and C.-K. Yeh, *J. Mater. Chem. B*, 2015, **3**, 5938–5941.
30 Y. Yang, Q. Li, X. Guo, J. Tu and D. Zhang, *Ultrason. Sonochem.*, 2020, **67**, 105096.
31 M. P. Walsh, R. V. Tikekar, N. Nitin and S. Wrenn, *J. Food Eng.*, 2021, **294**, 110410.
32 S. i. Umemura, N. Yumita, R. Nishigaki and K. Umemura, *Jpn. J. Cancer Res.*, 1990, **81**, 962–966.
33 L. A. Crum and R. A. Roy, *Science*, 1994, **266**, 233–234.
34 R. Hiller, S. J. Putterman and B. P. Barber, *Phys. Rev. Lett.*, 1992, **69**, 1182.

35 E. Beguin, S. Shrivastava, N. V. Dezhkunov, A. P. McHale, J. F. Callan and E. Stride, *ACS Appl. Mater. Interfaces*, 2019, **11**, 19913–19919.
36 Y. T. Didenko and K. S. Suslick, *Nature*, 2002, **418**, 394–397.
37 X. Xing, S. Zhao, T. Xu, L. Huang, Y. Zhang, M. Lan, C. Lin, X. Zheng and P. Wang, *Coord. Chem. Rev.*, 2021, **445**, 214087.
38 F. Gong, L. Cheng, N. Yang, Y. Gong, Y. Ni, S. Bai, X. Wang, M. Chen, Q. Chen and Z. Liu, *Nat. Commun.*, 2020, **11**, 1–11.
39 Y. Zhang, X. Zhang, H. Yang, L. Yu, Y. Xu, A. Sharma, P. Yin, X. Li, J. S. Kim and Y. Sun, *Chem. Soc. Rev.*, 2021, **50**, 11227–11248.
40 K. Kawamura, D. Hikosou, A. Inui, K. Yamamoto, J. Yagi, S. Saita and H. Kawasaki, *J. Phys. Chem. C*, 2019, **123**, 26644–26652.
41 A. Singh, R. Kukreti, L. Saso and S. Kukreti, *Molecules*, 2019, **24**, 1583.
42 C. Liang, J. Xie, S. Luo, C. Huang, Q. Zhang, H. Huang and P. Zhang, *Nat. Commun.*, 2021, **12**, 1–9.
43 A. Ma, H. Chen, Y. Cui, Z. Luo, R. Liang, Z. Wu, Z. Chen, T. Yin, J. Ni and M. Zheng, *Small*, 2019, **15**, 1804028.
44 Y. Li, J. Yang and X. Sun, *Front. Chem.*, 2021, **9**, 152.
45 C. Yang, Y. Zhang, Y. Luo, B. Qiao, X. Wang, L. Zhang, Q. Chen, Y. Cao, Z. Wang and H. Ran, *J. Mater. Chem. B*, 2020, **8**, 380–390.
46 D. Bertheloot, E. Latz and B. S. Franklin, *Cell. Mol. Immunol.*, 2021, **18**, 1106–1121.
47 F. Qu, P. Wang, K. Zhang, Y. Shi, Y. Li, C. Li, J. Lu, Q. Liu and X. Wang, *Autophagy*, 2020, **16**, 1413–1435.
48 L. Zhou, M. Huo, X. Qian, L. Ding, L. Yu, W. Feng, X. Cui and Y. Chen, *J. Nanobiotechnol.*, 2021, **19**, 1–15.
49 Y. Jin, Q. Zhou, J. Geng, Q. Meng, Z. Wei, M. Ding, J. Zhou, Y. Zeng, W. Cao and F. Liu, *Front. Pharmacol.*, 2021, 3584.
50 J. Hutcheson, R. Schlicher, H. Hicks and M. Prausnitz, *Ultrasound Med. Biol.*, 2010, **36**, 1008–1021.
51 M. Wu, Y. Ding and L. Li, *Nanoscale*, 2019, **11**, 19658–19683.
52 Y. Shi and T. Lammers, *Acc. Chem. Res.*, 2019, **52**, 1543–1554.
53 Z. Yang, D. Tao, W. Zhong, Z. Liu, L. Feng and M. Chen, *Biomaterials*, 2022, **280**, 121250.
54 N. R. Anderson, N. G. Minutolo, S. Gill and M. Klichinsky, *Cancer Res.*, 2021, **81**, 1201–1208.
55 W. Xie, S. Zhu, B. Yang, C. Chen, S. Chen, Y. Liu, X. Nie, L. Hao, Z. Wang and J. Sun, *Int. J. Nanomed.*, 2019, **14**, 9377.
56 S. K. Wculek, F. J. Cueto, A. M. Mujal, I. Melero, M. F. Krummel and D. Sancho, *Nat. Rev. Immunol.*, 2020, **20**, 7–24.
57 Y. Si, J. Yue, Z. Liu, M. Li, F. Du, X. Wang, Z. Dai, N. Hu, J. Ju and S. Gao, *Int. J. Nanomed.*, 2021, **16**, 1913.
58 R. J. Kishton, M. Sukumar and N. P. Restifo, *Cell Metab.*, 2017, **26**, 94–109.
59 C. Ji, J. Si, Y. Xu, W. Zhang, Y. Yang, X. He, H. Xu, X. Mou, H. Ren and H. Guo, *Theranostics*, 2021, **11**, 8587.
60 Z. Liu, J. Li, Y. Jiang and D. Wang, *Biomaterials*, 2019, **218**, 119251.
61 Q. Zhang, C. Bao, X. Cai, L. Jin, L. Sun, Y. Lang and L. Li, *Cancer Sci.*, 2018, **109**, 1330–1345.
62 D. Li, Y. Yang, D. Li, J. Pan, C. Chu and G. Liu, *Small*, 2021, **17**, 2101976.
63 Z. Yu, W. Cao, C. Han, Z. Wang, Y. Qiu, J. Wang, M. Wei, J. Wang, S. Zhang and S. Liu, *Front. Bioeng. Biotechnol.*, 2022, **10**, 796820.
64 H. Sun, W. Ge, X. Gao, S. Wang, S. Jiang, Y. Hu, M. Yu and S. Hu, *PLoS One*, 2015, **10**, e0137980.
65 K. Shono, Y. Mizobuchi, I. Yamaguchi, K. Nakajima, Y. Fujiwara, T. Fujihara, K. Kitazato, K. Matsuzaki, Y. Uto and O. Sampetrean, *Sci. Rep.*, 2021, **11**, 1–10.
66 L. C. Nene and T. Nyokong, *Photodiagnosis Photodyn. Ther.*, 2021, **36**, 102573.
67 N. Yumita, K.-i. Kawabata, K. Sasaki and S.-i. Umemura, *Ultrason. Sonochem.*, 2002, **9**, 259–265.
68 H.-J. Chen, X.-B. Zhou, A.-L. Wang, B.-Y. Zheng, C.-K. Yeh and J.-D. Huang, *Eur. J. Med. Chem.*, 2018, **145**, 86–95.
69 J. An, Y.-G. Hu, K. Cheng, C. Li, X.-L. Hou, G.-L. Wang, X.-S. Zhang, B. Liu, Y.-D. Zhao and M.-Z. Zhang, *Biomaterials*, 2020, **234**, 119761.
70 C. Komori, K. Okada, K. Kawamura, N. Suzuki, S. Chida and T. Suzuki, *Anticancer Res.*, 2009, **29**, 243–248.
71 J.-X. Zhu, W.-T. Zhu, J.-H. Hu, W. Yang, P. Liu, Q.-H. Liu, Y.-X. Bai and R. Xie, *Ultrasound Med. Biol.*, 2020, **46**, 2030–2043.
72 Y. Jiang, J. Kou, X. Han, X. Li, Z. Zhong, Z. Liu, Y. Zheng, Y. Tian and L. Yang, *Oxid. Med. Cell. Longevity*, 2017, **2017**, 8519169.
73 H. Abrahamse and M. R. Hamblin, *Biochem. J.*, 2016, **473**, 347–364.
74 X. Lin, J. Song, X. Chen and H. Yang, *Angew. Chem., Int. Ed.*, 2020, **59**, 14212–14233.
75 M. Liu, A. R. Khan, J. Ji, G. Lin, X. Zhao and G. Zhai, *J. Controlled Release*, 2018, **290**, 150–164.
76 Y. Zhang, A. R. Khan, X. Yang, Y. Shi, X. Zhao and G. Zhai, *J. Nanobiotechnol.*, 2021, **19**, 1–17.
77 S. Gao, Y. Jin, K. Ge, Z. Li, H. Liu, X. Dai, Y. Zhang, S. Chen, X. Liang and J. Zhang, *Adv. Sci.*, 2019, **6**, 1902137.
78 J. She, X. Zhou, Y. Zhang, R. Zhang, Q. Li, W. Zhu, Z. Meng and Z. Liu, *Adv. Healthcare Mater.*, 2021, **10**, 2001208.
79 G. Li, S. Wang, D. Deng, Z. Xiao, Z. Dong, Z. Wang, Q. Lei, S. Gao, G. Huang and E. Zhang, *ACS Nano*, 2020, **14**, 1586–1599.
80 H. He, Y. Lu, J. Qi, Q. Zhu, Z. Chen and W. Wu, *Acta Pharm. Sin. B*, 2019, **9**, 36–48.
81 H.-J. Chen, X.-R. Huang, X.-B. Zhou, B.-Y. Zheng and J.-D. Huang, *Chem. Commun.*, 2015, **51**, 4681–4684.
82 H. Chen, L. Liu, A. Ma, T. Yin, Z. Chen, R. Liang, Y. Qiu, M. Zheng and L. Cai, *Biomaterials*, 2021, **269**, 120639.
83 Y. Wang, Y. Liu, H. Wu, J. Zhang, Q. Tian and S. Yang, *Adv. Funct. Mater.*, 2019, **29**, 1805764.
84 Y. Zhang, H. Wang, X. Jia, S. Du, Y. Yin and X. Zhang, *J. Drug Targeting*, 2020, **28**, 195–203.
85 S. Liang, X. Deng, Y. Chang, C. Sun, S. Shao, Z. Xie, X. Xiao, P. a. Ma, H. Zhang and Z. Cheng, *Nano Lett.*, 2019, **19**, 4134–4145.
86 Y. Zhang, Y. Xu, D. Sun, Z. Meng, W. Ying, W. Gao, R. Hou, Y. Zheng, X. Cai and B. Hu, *Chem. Eng. J.*, 2020, **390**, 124521.

87 Z. Dong, L. Feng, Y. Hao, Q. Li, M. Chen, Z. Yang, H. Zhao and Z. Liu, *Chem*, 2020, **6**, 1391–1407.
88 D. Yang, A. Gulzar, G. Yang, S. Gai, F. He, Y. Dai, C. Zhong and P. Yang, *Small*, 2017, **13**, 1703007.
89 N. Shimizu, C. Ogino, M. F. Dadjour and T. Murata, *Ultrason. Sonochem.*, 2007, **14**, 184–190.
90 Y. Harada, K. Ogawa, Y. Irie, H. Endo, L. B. Feril Jr, T. Uemura and K. Tachibana, *J. Controlled Release*, 2011, **149**, 190–195.
91 F. Gao, G. He, H. Yin, J. Chen, Y. Liu, C. Lan, S. Zhang and B. Yang, *Nanoscale*, 2019, **11**, 2374–2384.
92 Q. Feng, X. Yang, Y. Hao, N. Wang, X. Feng, L. Hou and Z. Zhang, *ACS Appl. Mater. Interfaces*, 2019, **11**, 32729–32738.
93 X. Wang, X. Zhong, L. Bai, J. Xu, F. Gong, Z. Dong, Z. Yang, Z. Zeng, Z. Liu and L. Cheng, *J. Am. Chem. Soc.*, 2020, **142**, 6527–6537.
94 J. Cao, Y. Sun, C. Zhang, X. Wang, Y. Zeng, T. Zhang and P. Huang, *Acta Biomater.*, 2021, **129**, 269–279.
95 L. Cai, C. Hu, S. Liu, Y. Zhou, Z. Liu and M. Pang, *Bioconjugate Chem.*, 2021, **32**, 661–666.
96 F. Gong, L. Cheng, N. Yang, O. Betzer, L. Feng, Q. Zhou, Y. Li, R. Chen, R. Popovtzer and Z. Liu, *Adv. Mater.*, 2019, **31**, 1900730.
97 X. Lin, S. Liu, X. Zhang, R. Zhu, S. Chen, X. Chen, J. Song and H. Yang, *Angew. Chem.*, 2020, **132**, 1699–1705.
98 X. Pan, W. Wang, Z. Huang, S. Liu, J. Guo, F. Zhang, H. Yuan, X. Li, F. Liu and H. Liu, *Angew. Chem.*, 2020, **132**, 13659–13663.
99 P. Wang, X. Wang, L. Ma, S. Sahi, L. Li, X. Wang, Q. Wang, Y. Chen, W. Chen and Q. Liu, *Part. Part. Syst. Charact.*, 2018, **35**, 1700378.
100 J. Ouyang, L. Deng, W. Chen, J. Sheng, Z. Liu, L. Wang and Y.-N. Liu, *Chem. Commun.*, 2018, **54**, 2874–2877.
101 V. Catalano, A. Turdo, S. Di Franco, F. Dieli, M. Todaro and G. Stassi, *Semin. Cancer Biol.*, 2013, **8**, 7.
102 X. Zhong, X. Wang, L. Cheng, Y. a. Tang, G. Zhan, F. Gong, R. Zhang, J. Hu, Z. Liu and X. Yang, *Adv. Funct. Mater.*, 2020, **30**, 1907954.
103 H. Lei, X. Wang, S. Bai, F. Gong, N. Yang, Y. Gong, L. Hou, M. Cao, Z. Liu and L. Cheng, *ACS Appl. Mater. Interfaces*, 2020, **12**, 52370–52382.
104 N. W. S. Kam, M. O'Connell, J. A. Wisdom and H. Dai, *Proc. Natl. Acad. Sci. U. S. A.*, 2005, **102**, 11600–11605.
105 C. Dai, S. Zhang, Z. Liu, R. Wu and Y. Chen, *ACS Nano*, 2017, **11**, 9467–9480.
106 N. Behzadpour, A. Ranjbar, N. Azarpira and N. Sattarahmady, *Ultrasound Med. Biol.*, 2020, **46**, 2322–2334.
107 S. Yang, X. Wang, P. He, A. Xu, G. Wang, J. Duan, Y. Shi and G. Ding, *Small*, 2021, **17**, 2004867.
108 N. Wu, C.-H. Fan and C.-K. Yeh, *Drug Discovery Today*, 2022, **27**, 1590–1603.
109 Z. Zeng, C. Zhang, S. He, J. Li and K. Pu, *Adv. Mater.*, 2022, 2203246.
110 X. Hu, S. Zhai, G. Liu, D. Xing, H. Liang and S. Liu, *Adv. Mater.*, 2018, **30**, 1706307.
111 Y. Liu, G. Wan, H. Guo, Y. Liu, P. Zhou, H. Wang, D. Wang, S. Zhang, Y. Wang and N. Zhang, *Nano Res.*, 2017, **10**, 834–855.
112 J. Tang, X. Zhang, L. Cheng, Y. Liu, Y. Chen, Z. Jiang and J. Liu, *Bioact. Mater.*, 2022, **15**, 355–371.
113 W. Um, P. K. Ek, Y. Song, J. Lee, J. Y. An, H. Joo, D. G. You and J. H. Park, *Carbohydr. Polym.*, 2021, **273**, 118488.
114 Y. Zhang, N. Qiu, Y. Zhang, H. Yan, J. Ji, Y. Xi, X. Yang, X. Zhao and G. Zhai, *Biomater. Sci.*, 2021, **9**, 3989–4004.
115 S.-G. Wu and J.-Y. Shih, *Mol. Cancer*, 2018, **17**, 1–14.
116 P. Zhang, L. Zhang, J. Wang, L. Zhu, Z. Li, H. Chen and Y. Gao, *Carbohydr. Polym.*, 2021, **274**, 118655.
117 C. Dong, Q. Jiang, X. Qian, W. Wu, W. Wang, L. Yu and Y. Chen, *Nanoscale*, 2020, **12**, 5587–5600.
118 R. Li, Z. Chen, Z. Dai and Y. Yu, *Cancer Biol. Med.*, 2021, **18**, 388.
119 Y. Yang, J. Tu, D. Yang, J. L. Raymond, R. A. Roy and D. Zhang, *Curr. Pharm. Des.*, 2019, **25**, 401–412.
120 J. Zhu, Y. Wang, P. Yang, Q. Liu, J. Hu, W. Yang, P. Liu, F. He, Y. Bai and S. Gai, *Colloids Surf., B*, 2021, **197**, 111358.
121 L. Hong, A. M. Pliss, Y. Zhan, W. Zheng, J. Xia, L. Liu, J. Qu and P. N. Prasad, *Nanomaterials*, 2020, **10**, 2058.
122 Y. Zheng, Z. Li, Y. Yang, H. Shi, H. Chen and Y. Gao, *Phytomedicine*, 2021, **93**, 153788.
123 A. Sundaram, L. Peng, L. Chai, Z. Xie, J. S. Ponraj, X. Wang, G. Wang, B. Zhang, G. Nie and N. Xie, *Nanoscale*, 2020, **12**, 21497–21518.
124 S. Bai, N. Yang, X. Wang, F. Gong, Z. Dong, Y. Gong, Z. Liu and L. Cheng, *ACS Nano*, 2020, **14**, 15119–15130.
125 X. Ren, D. Chen, Y. Wang, H. Li, Y. Zhang, H. Chen, X. Li and M. Huo, *J. Nanobiotechnol.*, 2022, **20**, 1–18.
126 X. Qiao, L. Xue, H. Huang, X. Dai, Y. Chen and H. Ding, *J. Nanobiotechnol.*, 2022, **20**, 1–17.
127 S. Fu, R. Yang, J. Ren, J. Liu, L. Zhang, Z. Xu, Y. Kang and P. Xue, *ACS Nano*, 2021, **15**, 11953–11969.
128 S. Liang, X. Xiao, L. Bai, B. Liu, M. Yuan, P. a. Ma, M. Pang, Z. Cheng and J. Lin, *Adv. Mater.*, 2021, **33**, 2100333.
129 J. Liu, S. Fu, J. Xie, J. Zhang, J. Pan, C. Chu, G. Liu and S. Ju, *Biosensors*, 2022, **12**, 255.
130 K. M. Nowak, M. R. Schwartz, V. R. Breza and R. J. Price, *Cancer Lett.*, 2022, 215592.
131 N. Tao, H. Li, L. Deng, S. Zhao, J. Ouyang, M. Wen, W. Chen, K. Zeng, C. Wei and Y.-N. Liu, *ACS Nano*, 2021, in press.
132 X. Wei, Z. Feng, J. Huang, X. Xiang, F. Du, C. He, M. Zhou, L. Ma, C. Cheng and L. Qiu, *ACS Appl. Mater. Interfaces*, 2021, **13**, 32810–32822.
133 J. Huang, Z. Xiao, Y. An, S. Han, W. Wu, Y. Wang, Y. Guo and X. Shuai, *Biomaterials*, 2021, **269**, 120636.
134 J. Luo, X. Wang, Z. Shi, Y. Zeng, L. He, J. Cao, Y. Sun, T. Zhang and P. Huang, *J. Nanobiotechnol.*, 2022, **20**, 1–17.
135 X. Lin, R. Huang, Y. Huang, K. Wang, H. Li, Y. Bao, C. Wu, Y. Zhang, X. Tian and X. Wang, *Int. J. Nanomed.*, 2021, **16**, 1889.
136 Y. Tan, S. Yang, Y. Ma, J. Li, Q. Xie, C. Liu and Y. Zhao, *Int. J. Nanomed.*, 2021, **16**, 3241.

137 X. Li, J. F. Lovell, J. Yoon and X. Chen, *Nat. Rev. Clin. Oncol.*, 2020, **17**, 657–674.
138 T. Shang, X. Yu, S. Han and B. Yang, *Biomater. Sci.*, 2020, **8**, 5241–5259.
139 X. Jiao, L. Sun, W. Zhang, J. Ren, L. Zhang, Y. Cao, Z. Xu, Y. Kang and P. Xue, *Biomaterials*, 2021, **272**, 120787.
140 G. Li, X. Zhong, X. Wang, F. Gong, H. Lei, Y. Zhou, C. Li, Z. Xiao, G. Ren and L. Zhang, *Bioact. Mater.*, 2022, **8**, 409–419.
141 Z. Liu, J. Li, W. Chen, L. Liu and F. Yu, *Biomaterials*, 2020, **232**, 119685.